Heliyon 10 (2024) e26843

Contents lists available at ScienceDirect

Heliyon

journal homepage: www.cell.com/heliyon

Research article

Pyrazole-based and N,N-diethylcarbamate functionalized some novel aurone analogs: Design, synthesis, cytotoxic evaluation, docking and SAR studies, against AGS cancer cell line

Ekta Lathwal [a,b], Sanjeev Kumar [a,c], Pranab Kumar Sahoo [d], Sushmita Ghosh [d], Sutapa Mahata [d], Vilas D. Nasare [d], Ravikumar Kapavarapu [e], Suresh Kumar [a,*]

[a] Department of Chemistry, Kurukshetra University, Kurukshetra, 136119, Haryana, India
[b] Govt. College, Tigaon, Faridabad, 121101, Haryana, India
[c] PGT Chemistry, KendriyaVidyalaya Kokrajhar, Assam, 783370, India
[d] Department of Pathology and Cancer Screening, Chittaranjan National Cancer Institute, 37, S.P. Mukherjee Road, Kolkata, India
[e] Department of Pharmaceutical Chemistry and Phytochemistry, Nirmala College of Pharmacy, Atmakur, Mangalagiri, Andhra Pradesh, India

ARTICLE INFO

Keywords:
Aurone
Diethylcarbamate
Pyrazole
Synthesis
AGS cell line
Molecular docking

ABSTRACT

The present study involves the design, synthesis, and biological evaluation of a series of thirty-three, pyrazole-based and N,N-diethylcarbamate functionalized, novel aurone analogs, against AGS cancer cell line. These novel aurone analogs are obtained from the reaction of pyrazole-based 6-hydroxyaurones with diethyl carbamoyl chloride using mild basic reagent. The cytotoxic activities of these compounds were evaluated against a human gastric adenocarcinoma cell line (AGS) and disclosed some potential outcomes as several analogs were found to have cytotoxicity better than the reference drugs Oxaliplatin and Leucovorin. The structure-activity relationship (SAR) study further unveiled the critical role of replacing the hydroxyl group in ring A with a carbamoyl group for cytotoxic activity. Among these aurone analogs, **8e** and **8f**, with $\mathbf{IC_{50}}$ values of **6.5 ± 0.024 μM** and **6.6 ± 0.035 μM**, respectively, are identified as the most active compounds. Molecular docking studies were conducted against HER2, a human epidermal growth factor involved in gastric and ovarian cancer, to investigate the binding interactions between the compounds and the protein **HER2**, where**7e** and **8e** exhibited maximum interactions.

1. Introduction

Heterocyclic compounds or heterocycles are widely spread in all living and non-living organisms and is the most prominent class of organic compounds contributing to medicinal and biological chemistry. Heterocycles possess a broad spectrum of applications in different fields [1–6] and pyrazole containing heterocyclic compounds with a wide variety of biological applications is one of them [7–15] that have played an important role in the design and synthesis of many natural and synthetic medicines [16,17]. Pyrazole-based compounds are found to be associated with diverse biological activities [18,19], like anti-inflammatory [20], analgesic [21,22], COX-2 inhibitor [23–25], tyrosine phosphatase 1B (PTP1B) inhibitors [26], antipyretic [27], antiobesity [28], CB1 cannabinoid receptor antagonists [29,30], anticancer [31], antibacterial [32], antiviral [33], antichagasic [34], lesishmanicidal [35], pesticidal [36] and

* Corresponding author. Department of Chemistry, Kurukshetra University; Kurukshetra, Haryana, India.
E-mail addresses: suresh_dua47@rediffmail.com, duaskchem@gmail.com (S. Kumar).

https://doi.org/10.1016/j.heliyon.2024.e26843
Received 10 February 2024; Accepted 20 February 2024
Available online 24 February 2024

antitumoral [37,38] activities. Some of the prominent pyrazole based drugs [39] are ramifenazone [40], deracoxib [41], celecoxib [42], rimonabant [43], pyrazofurin [44], difenamizole [45], tartrazine [46] and sulfaphenazole [47](Fig. 1).

Aurone, a minor class of flavonoids, are secondary metabolites widespread among the higher plants and serving many physiological functions [48,49]. Besides this flavone, flavonol, flavanone, flavanonol, anthocyanin, catechin and chalcone are the other subclasses of flavonoids [50]. Aurone, chemically known as 2-benzylidenebenzofuran-3(2*H*)-one [51], are tricyclic compounds that consist of heterocyclic benzofuranone moiety bridging with phenyl ring by carbon-carbon exo-cyclic double bond and are structural isomers of flavones [52] (Fig. 2). Aurones impart a golden yellow color to some fruits and flower petals [53], do photoprotection, and as phytoalexins protect plants from rot, insect, and various other microbial infections [54]. Natural aurones, and their semisynthetic and synthetic analogs have shown some significant and versatile biological activities, including anti-tumor/anti-cancer [55,56], anti-diabetic [57], antioxidant [58], antiparasitic [59], antibacterial [60], insect antifeedant [61], antitubercular [62], neuroprotective [63], anti-inflammatory [64], antiviral [64], antimalarial [65], antioxidant [66], antibiofim activities [67], alleviating allergic manifestation [68], inhibitors of enzymes such as monoamine oxidase A and B [69,70], cyclin-dependent kinase [71], acetylcholinesterase [72], tyrosinase in melanin-related disorders [73], as antiobesity agents [74,75] in living organisms ranging from protozoans to mammals [76].

Aurones have been identified as newer and potential therapeutic agents for treating cancer because of their interactions at the different molecular levels including modulation of drug efflux pumps such as P-gp/ABCB1 and BCRP/ABCG2 [77], modifiers of adenosine-receptor interactions [78], inhibition of cyclin-dependent kinase (CDK), inhibition of human sphingosine kinase (SphK) and interaction with tubulin binding site leading to arrest in cell cycle progression [75,79], cancer chemoprevention by antioxidant mechanisms such as inducers of cytoprotective NAD(P)H:quinone oxidoreductase 1 (NQO1) activity, CTSB inhibition activity [80] and exhibited potent DNA strand-scission activity [81]. A literature study has confirmed that introducing the selected group at C-6 (ring A) in place of the hydroxyl group of aurone molecule can enhance their biological profile [82–85]. The significance of heterocycles in the treatment of gastric cancer inspired us to explore some potential outcomes from aurone by introducing N,N-diethyl carbamate group in place of the hydroxyl group at C-6 position of previously reported pyrazole-based aurones from our lab [86]. Incorporation of the N,

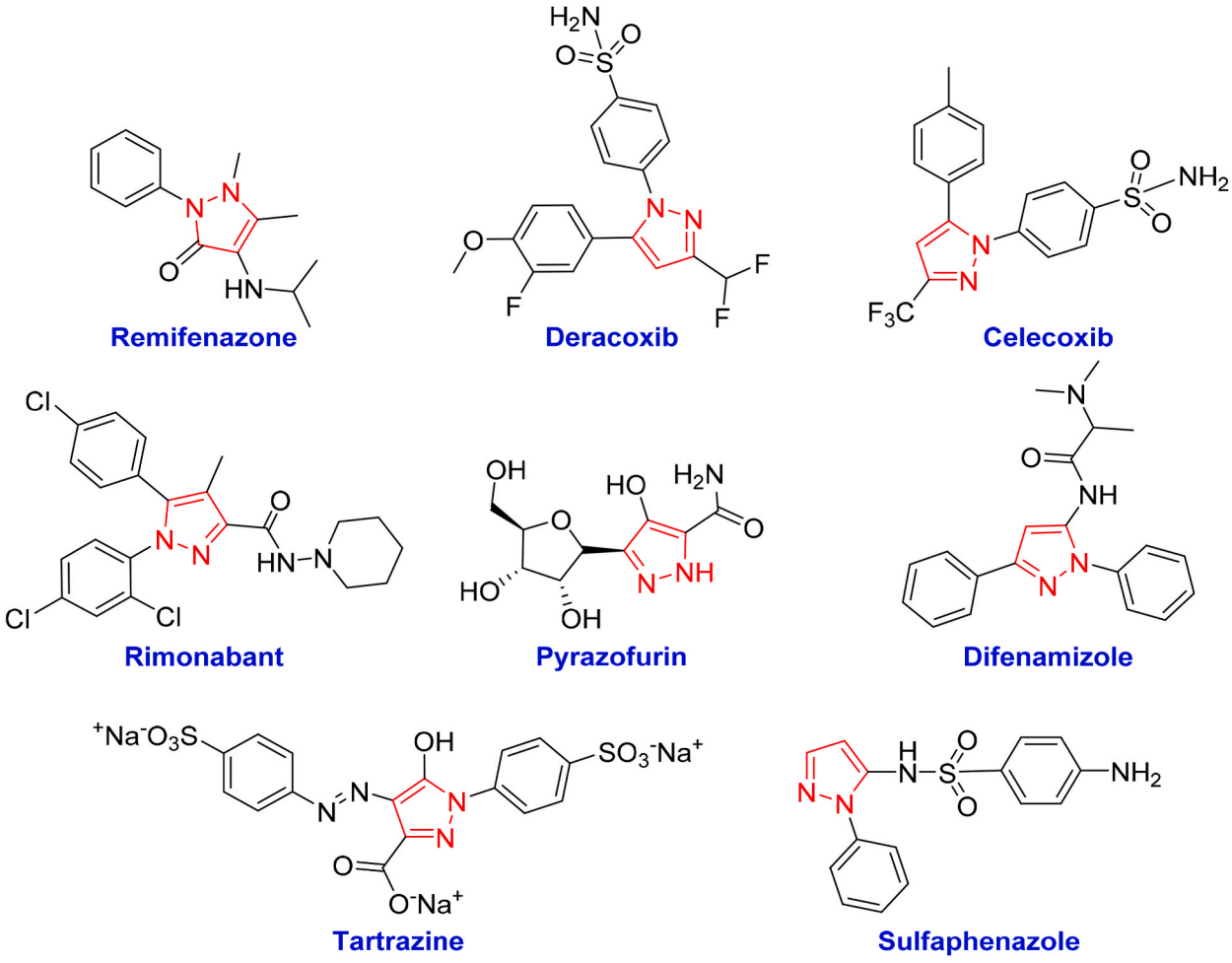

Fig. 1. Some pyrazole-based market available drugs.

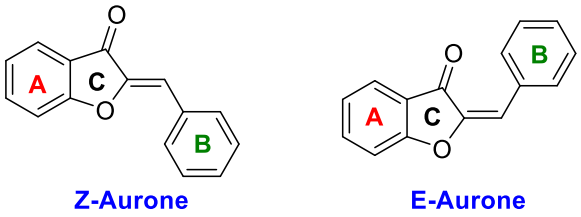

Fig. 2. Stereoisomeric forms of aurone.

N-diethylcarbamate group enhances the alignment of drug molecules within the active sites of various enzymes, ultimately improving their therapeutic potential. N,N-Diethyl carbamate scaffold has frequently been used by the medicinal chemists to increase the biological potency of many compounds [87,88] and therefore we used here in designing for these novel aurone analogs.

2. Results and discussion

2.1. Chemistry

In continuation of our ongoing research on synthesizing and exploring novel aurones or aurone-based heterocycles for their biological or medicinal significance, we synthesized thirty-three pyrazole-based novel aurone analogs **7(a–k)**, **8(a–k)**, **9(a–k)**, bearing N, N-dietylcarbamate functionality at the 6th position in ring A, in 88–97% of yield. These novel aurones were obtained by functionalizing the hydroxyl group at C-6 position of previously reported pyrazole-based aurones from our lab **4(a–k)**, **5(a–k)**, **6(a–k)**(Scheme 1), with N,N-diethylcarbamate. As we functionalized the previously reported *Z*-aurones [86] therefore *Z*-configuration is also assigned to these novel aurone analogs.

Structures of all these compounds were confirmed based on their IR, ^{1}H NMR, ^{13}C NMR, and HRMS data. In ^{1}H NMR spectra of all the synthesized analogs **7–9(a–k)**, a distinct singlet peak in the δ 7.17–6.63 ppm region appeared confirming the presence of olefinic proton of exocyclic double bond. Additionally, the proton present in the pyrazole moiety resonated in the range of δ 9.23–8.65 ppm. The ^{13}C NMR spectra showed a downfield peak in the δ 184.52–181.71 ppm region for carbonyl carbon. The structures of the hybrid compounds were further confirmed by analysing their HRMS data, which showed corresponding protonated $[M+H]^{+}$ molecular ion peaks.

After successful characterization, all the newly synthesized aurone analogs were screened for their cytotoxic activity against human gastric adenocarcinoma cell line, and some compounds exhibited a significant cytotoxic activity even better than the reference drugs oxaliplatin and leucovorin (Table 1). A structure-activity relationship study for cytotoxic activity against the AGS cell line was also

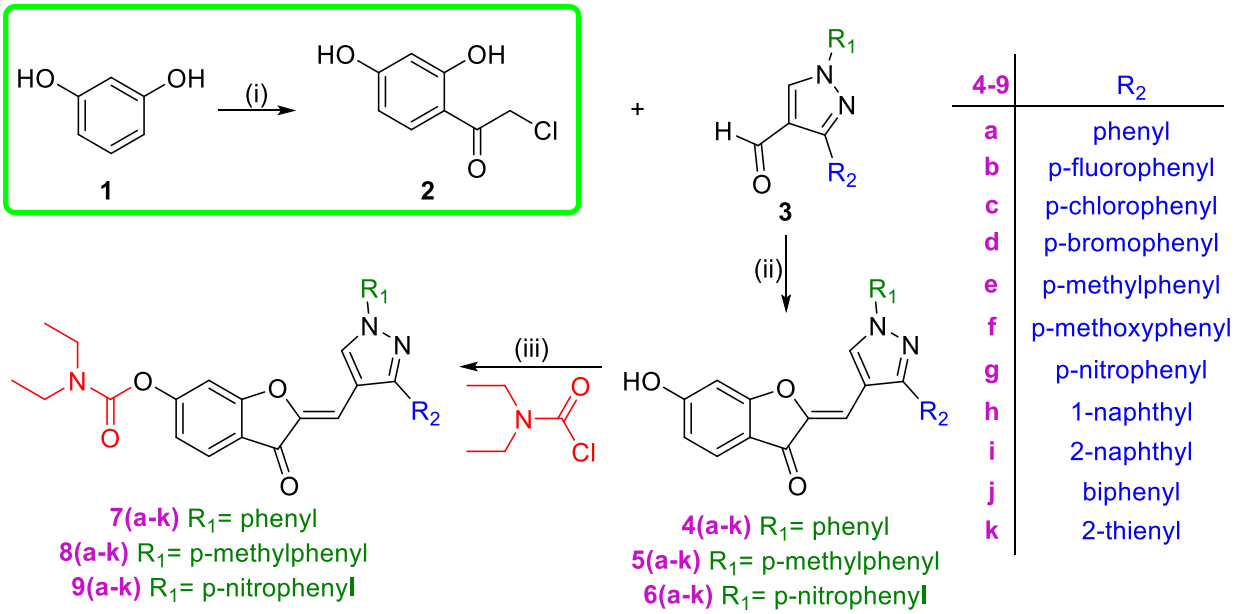

Scheme 1. Synthetic protocol for Pyrazole-based and N,N-diethylcarbamate functionalized novel aurones; Reagents and Conditions: (i) chloro acetylchloride, $AlCl_3$, ethyl acetate, r.t., 6 h then 50 ^{0}C, 2 h; (ii) activated $Ba(OH)_2$, DMSO, 80 ^{0}C, 5–6 h; (iii) K_2CO_3, acetone, reflux, 3–4 h.

made considering novel analogs and their corresponding pyrazole-based hydroxy aurone derivatives, reported previously. Molecular docking, is a key computational tool for predicting the binding mode of small molecules to a protein in terms of interaction energies and has frequently been used in drug designing and development [89]. Recent studies have confirmed the involvement of HER2 protein, a human epidermal growth factor in gastric and gastroesophageal cancer [90,91]. We performed the Swiss Target prediction studies and from this study we came to know that the designed Pyrazole-based and N,N-diethylcarbamate functionalized novel aurone analogs find structural similarity with known active human epidermal growth factor (HER2). As the designed molecules were found very active against AGS cancer cell line based on *in-vitro* studies, therefore molecular docking studies were conducted against HER2 receptor to investigate the binding interactions between the compounds and the receptor protein to have some useful insight and to correlate the *in-silico* results with the *in-vitro* results.

2.2. Structure-activity relationship (SAR) study

All the aurone analogs were evaluated for their antiproliferative activity against AGS cancer cell line using oxaliplatin and leucovorin as the reference drugs. This study was aimed to find the impact of replacing the hydroxyl group at the 6th position with the carbamate group in the pyrazole-based aurone towards cytotoxic activity against the AGS cell line for all the compounds and to have a systematic structure-activity relationship for the cytotoxic activity against AGS cancer cell line of these newly synthesized 6-*O*-functionalized N,N-diethycarbamates of pyrazole-based 6-hydroxyaurones **7(a–k)**, **8(a–k)** and **9(a–k)** in comparison with the previously reported pyrazole-based 6-hydroxyaurones **4(a–k)**, **5(a–k)** and **6(a–k)** (Table 1). Most of the synthesized compounds with carbamate group displayed stronger activity than the corresponding compounds **4(a–k)**, **5(a–k)** and **6(a-k)**with a hydroxyl group at ring A of the scaffold with few exceptions as shown in Table 1. All the compounds with the carbamate group and having p-methyl phenyl functionality on 1st position of pyrazole moiety showed better activity when compared with the corresponding hydroxy group-containing pyrazoleaurones i.e. **8(a–k)**>**5(a–k)** and carbamate functionalized aurone analogs of other two series i.e. **8(a–k)**>**7(a–k)**> **9(a–k)**. However, carbamate-functionalized aurones having phenyl functionality on the 1st position of pyrazole moiety also showed better cytotoxic activity compared with the corresponding hydroxy group-containing pyrazole aurones (**7(a–k)**>**4(a–k)**) but have few exceptions. In contrast for all the compounds of series having *p*-nitrophenyl functionality on the 1st position of pyrazole moiety, the functionalization of the hydroxyl group with carbamate functional group leads to a substantial decrease in cytotoxic activity i.e. **6(a–l)**>**9(a–l)**(Fig. 3). Thus we may conclude that carbamate functionality on ring A and the p-methyl phenyl group on the 1st position of the pyrazole ring is favorable for the cytotoxic activity against the AGS cancer cell line. Among all compounds, tested for cytotoxic activity, the majority of compounds exhibited moderate to strong activity but **7(e,f)**, **8a**, **8(d–f),** and **8(i–k)** showed stronger cytotoxic activity even better than all previously reported compounds **4(a–k)**, **5(a–k)**, and **6(a–k),** and reference drugs oxaliplatin and leucovorin (Table 1). Whereas compounds with the *p*-nitrophenyl group at 1st position of the pyrazole ring showed moderate to weak anticancer activity. Thus an electron-donating group at the *p*-position of the phenyl ring linked to the 1st position of the pyrazole ring leads to an increase in antiproliferative activity than the corresponding electron-withdrawing group. For the halogen group at the *p*-position the order of activity is Br > Cl > F i.e. for Br **(8d > 7d > 9d)** > for Cl **(8c > 7c > 9c)** > for F **(8b > 7b > 9b)** (Fig. 3). Compound **8e**, which contain methyl group at *p*-position of both the phenyl ring of pyrazole nucleus, emerged out the most potent cytotoxic agent in this study. Moreover, substituting the hydroxy group in 4e with a carbamate group (7e) significantly enhances the antiproliferative activity to around nearly five times. Similar observations were noted from 5e to 8e, where activity enhancement was approximately four times. Aurone analogs bearing an electron-releasing group, such as p-methyl and *p*-methoxy on the phenyl ring at the 3-position of the pyrazole ring, exhibited activity in the order of 8e > 8f > 7e > 7f > 9e > 9f, in which 8(e, f) and 7(e, f) showed highest activity (see Table 1).

Table 1
Cytotoxic activity against AGS cancer cell line.

Compounds	[a]4	[a]5	[a]6	[b]7	[b]8	[b]9
	[c]IC_{50} (μM)			[c]IC_{50} (μM)		
a	54.4 ± 0.165	33.9 ± 0.083	36.0 ± 0.058	34.5 ± 0.020	23.5 ± 0.070	49.3 ± 0.016
b	53.1 ± 0.023	36.3 ± 0.050	44.2 ± 0.494	39.4 ± 0.040	30.6 ± 0.027	66.8 ± 0.035
c	54.6 ± 0.066	33.4 ± 0.135	42.8 ± 0.120	38.6 ± 0.048	**29.7 ± 0.040**	62.3 ± 0.035
d	53.1 ± 0.023	32.7 ± 0.032	34.9 ± 0.057	37.9 ± 0.070	**24.9 ± 0.021**	61.3 ± 0.017
e	48.5 ± 0.016	**25.0 ± 0.025**	40.1 ± 0.039	**10.3 ± 0.022**	**6.5 ± 0.024**	42.7 ± 0.037
f	61.1 ± 0.032	**28.3 ± 0.022**	43.7 ± 0.018	**17.8 ± 0.026**	**6.6 ± 0.035**	44.6 ± 0.026
g	42.1 ± 0.029	33.6 ± 0.014	**25.1 ± 0.102**	41.5 ± 0.070	32.0 ± 0.019	74.7 ± 0.081
h	80.7 ± 0.063	43.3 ± 0.066	60.1 ± 0.039	42.8 ± 0.014	30.7 ± 0.017	71.6 ± 0.047
i	39.4 ± 0.040	**27.0 ± 0.049**	33.6 ± 0.062	33.6 ± 0.062	**21.3 ± 0.034**	47.7 ± 0.020
j	61.9 ± 0.023	38.2 ± 0.029	45.7 ± 0.090	35.5 ± 0.031	**24.3 ± 0.077**	50.6 ± 0.040
k	60.9 ± 0.033	34.3 ± 0.055	44.9 ± 0.022	36.7 ± 0.082	**24.4 ± 0.082**	52.9 ± 0.022
Oxaliplatin	**29.8 ± 0.010**					
Leucovorin	**30.8 ± 0.096**					

[a]Previously reported compounds **4(a–k)**, **5(a–k)** and **6(a–k)**.
[b]Newly synthesized compounds **7(a–k)**, **8(a–k)** and **9(a–k)**.
[c]IC_{50}: Each data point represents the mean from three different experiments performed in triplicates. AGS cancer cell line was used.

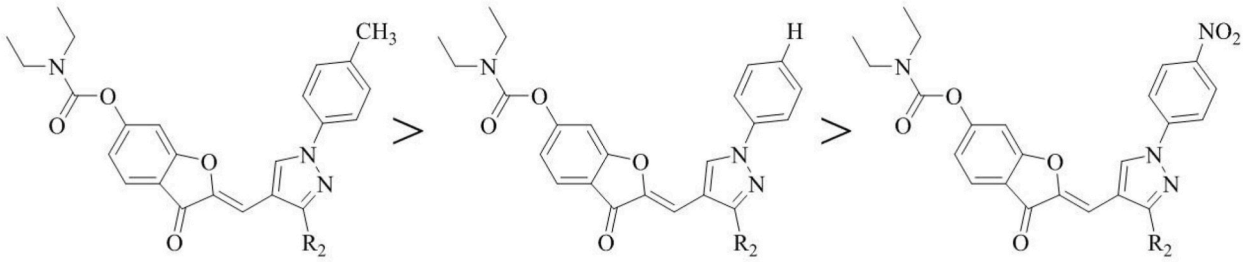

R_2 = 4-Me Phenyl > 4-OMe Phenyl > 2-Naphthyl > Phenyl > Biphenyl > 2-Thienyl > 4-Br Phenyl, 4-Cl Phenyl > 4-F Phenyl > 1-Naphthyl > 4-NO_2 Phenyl

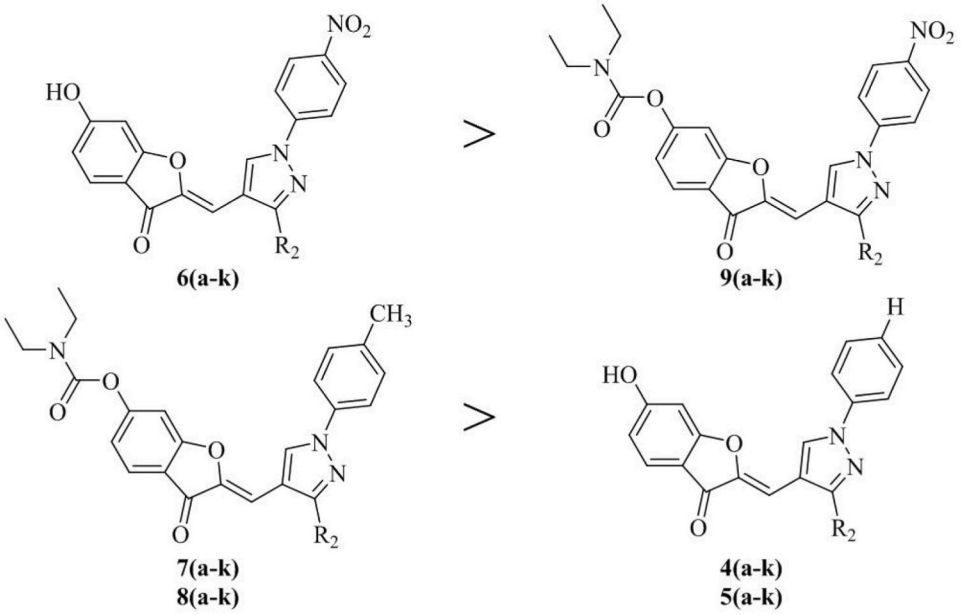

Fig. 3. SAR studies of pyrazole-based 6-hydroxyaurones and their 6-*O*-functionalized N,N-diethycarbamate analogs for the cytotoxic activity.

2.3. Assessment of morphological changes

AGS cells, either untreated or treated with N,N-diethylcarbamate-functionalized, pyrazole-based novel aurone analogs at various concentrations for 24 hours, were examined and images were captured with an inverted phase contrast microscope (Leica DMi1, Leica Microsystems, India) (Fig. 4). Remarkably, the treated cells exhibited significant alterations in their morphologies.. Fig. 4, illustrates the effects of treating AGS cell lines with different concentrations (0, 5, 10, 25, 50, and 100 μM) of the most active compound **8e**.

3. Conclusion

In this study, we have synthesized a total of thirty-three novel carbamate derivatives of pyrazole-based 6-hydroxyaurones under milder reaction conditions and evaluated them for their antiproliferative activity against human gastric adenocarcinoma (AGS) cell line. All the compounds exhibited moderate to very good cytotoxic activity with some significant outcomes in SAR studies. The structure-activity relationship analysis revealed that the carbamoyl group in place of the hydroxyl group in ring A is crucial for cytotoxic activity. Notably, compounds **7(e,f)**, **8(c–f)**, and **8(i–k)** demonstrated some outstanding antiproliferative activity towards the AGS cell line even better than the reference drugs oxaliplatin and leucovorin. Compound **8e**, containing methyl group at the *p*-position of both the phenyl ring of pyrazole nucleus emerged as the best cytotoxic agent in this study, thus emphasizing the significance of having an electron-releasing *p*-methyl group for enhancing anticancer activity. Additionally, molecular docking studies demonstrated that **7e**, **8e**, and **9c** exhibited significant binding interactions with HER2 human protein, involved in gastric cancer. The *in-silico* and *in-vitro* results of these compoundssupport each other. Thus these compounds may be further explored for their potential use as anticancer agents for gastric cancer.

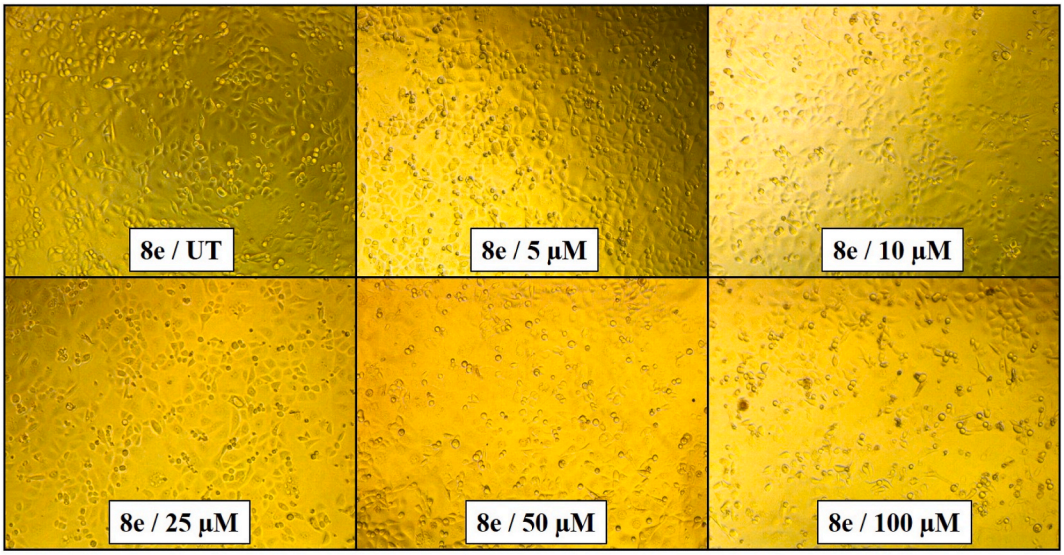

Fig. 4. Representative cell morphology of human gastric adenocarcinoma cell line after 24h drug treatment with **8e**. *UT: Untreated cell line.

4. Experimental

4.1. Chemistry

4.1.1. General

The solvents used were initially dried using the reported standard procedures and then used. The chemicals obtained from commercial sources were used as such without further purification available. A mixture of chloroform and methanol was used as eluent, to monitor the reactions by thin layer chromatography (TLC). For TLC, silica gel on F 254 aluminium plates was used and visualized in U. V lamp. Melting points were determined by an electrical melting point apparatus in open glass capillaries and may be uncorrected. IR spectra were recorded on ABB MB 3000 DTGS IR instrument using the KBr pellet techniques. ^{1}H NMR spectra were recorded at 400 MHz or 500 MHz, and ^{13}C NMR spectra were registered at 100 MHz or 125 MHz, using deuterated dimethyl sulfoxide (DMSO-d_6) or deuterated chloroform ($CDCl_3$) as solvent, and tetramethylsilane (TMS) as internal standard. Chemical shifts, δ are reported in parts per million (ppm) and coupling constant, *J* in hertz (Hz). High-resolution mass spectra (HRMS) were obtained from a MicroMass ESI-TOF MS spectrometer. Multiplicities of the NMR spectrum are described as singlet (s), doublet (d), doublet of doublet (dd), triplet (t), quartet (q), multiplet (m), and for IR the peaks are assigned as strong (s), medium (m), broad (br), symmetric (*sym.*) and asymmetric (*asym.*). Pyrazole-based aurones **4(a–k)**, **5(a–k)** and **6(a-k)** used in the reaction were synthesized in the laboratory as mentioned in our previous publication using suitable pyrazole aldehydes [86,92,93].

4.1.2. Synthesis of 6-O-functionalized N,N-diethycarbamate of pyrazole-based 6-hydroxyaurones 7(a-k), 8(a-k), and 9(a–k)

General procedure: pyrazole-based 6-hydroxyaurone (1.00 mmol) and acetone (15 mL) were mixed in a 100 mL round bottom flask. Then K_2CO_3 (2.00 mmol) and diethylcarbamoyl chloride (1.50 mmol) were added to the reaction mixture and refluxed for 3–4 h. The progress of the reaction was monitored by TLC. After the completion of the reaction, the solvent was removed by distillation, and the concentrated reaction mixture was poured on ice-cold water. The precipitates formed were filtered off using the suction machine, washed with water, and recrystallized from ethanol if required.

4.2. Spectral data

4.2.1. (Z)-2-((1,3-diphenyl-1H-pyrazol-4-yl)methylene)-3-oxo-2,3-dihydrobenzofuran-6-yl diethylcarbamate (7a)

Yield: 94 %; Yellow solid; mp: 196–198 °C; IR (KBr), ν (cm^{-1}): 1728 and 1643 (C=O), 1597 (C=C), 1535 (C=N); ^{1}H NMR (400 MHz, $CDCl_3$) δ (ppm): 8.74 (s, 1H, pyrazole), 7.87 (d, J = 7.6 Hz, 2H, Ar), 7.79 (d, J = 8.4 Hz, 1H, Ar), 7.74–7.72 (m, 2H, Ar), 7.55–7.47 (m, 5H, Ar), 7.37 (t, J = 7.2 Hz, 1H, Ar), 7.32 (d, J = 1.8 Hz, 1H, Ar), 7.06 (s, 1H, =CH), 6.98 (dd, J = 1.8 Hz, J = 8.4 Hz, 1H, Ar), 3.45 (q, J = 7.2 Hz, 4H, CH_2), 1.42–1.29 (m, 6H, CH_3); ^{13}C NMR (125 MHz, $CDCl_3$) δ (ppm): 182.43, 166.13, 158.42, 154.78, 152.99, 147.19, 139.61, 132.00, 130.29, 129.67, 129.01, 128.99, 128.91, 127.40, 125.38, 119.64, 119.35, 117.38, 113.99, 106.40, 104.70, 42.64, 42.26, 14.40, 13.42.

4.2.2. (Z)-2-((3-(4-fluorophenyl)-1-phenyl-1H-pyrazol-4-yl)methylene)-3-oxo-2,3-dihydrobenzofuran-6-yl diethylcarbamate (7b)

Yield: 90 %; Yellow solid; mp: 193–195 °C; IR (KBr) ν (cm^{-1}): 1714 and 1647 (C=O), 1597 (C=C), 1528 (C=N); ^{1}H NMR (500 MHz, $CDCl_3$) δ (ppm): 8.71 (s, 1H, pyrazole), 7.84 (d, J = 8.5 Hz, 2H, Ar), 7.77 (d, J = 8.5 Hz, 1H, Ar), 7.71–7.68 (m, 2H, Ar), 7.52 (t, J = 7.5

Hz, 2H, Ar), 7.37 (t, J = 7.5 Hz, 1H, Ar), 7.31 (s, 1H, Ar), 7.20 (t, J = 8.5 Hz, 2H, Ar), 6.97–6.96 (m, 2H, Ar, =CH), 3.48–3.41 (m, 4H, CH_2), 1.29–1.27 (m, 6H, CH_3); ^{13}C NMR (125 MHz, $CDCl_3$) δ (ppm): 182.43, 166.13, 163.32 (d, J = 248.5 Hz), 158.46, 153.74, 152.98, 147.23, 139.50, 130.79, 130.72, 130.30, 129.70, 127.49, 125.40, 119.60, 117.45, 116.15, 115.98, 113.87, 106.42, 104.24, 42.65, 42.26, 14.41, 13.43.

4.2.3. (Z)-2-((3-(4-chlorophenyl)-1-phenyl-1H-pyrazol-4-yl)methylene)-3-oxo-2,3-dihydrobenzofuran-6-yl diethylcarbamate (7c)

Yield: 95 %; Yellow solid; mp: 199–201 °C; IR (KBr) ν (cm^{-1}): 1720 and 1643 (C=O), 1597 (C=C), 1528 (C=N); ^{1}H NMR (400 MHz, $CDCl_3$) δ (ppm): 8.70 (s, 1H, pyrazole), 7.84–7.83 (m, 2H, Ar), 7.77 (d, J = 8.5 Hz, 1H, Ar), 7.66 (d, J = 8.0 Hz, 2H, Ar), 7.53–7.47 (m, 4H, Ar), 7.39–7.36 (m, 1H, Ar), 7.31 (d, J = 2.0 Hz, 1H, Ar), 6.97–6.95 (m, 2H, Ar, =CH), 3.48–3.40 (m, 4H, CH_2), 1.29–1.26 (m, 6H, CH_3); ^{13}C NMR (125 MHz, $CDCl_3$) δ (ppm): 182.41, 166.14, 158.48, 153.44, 152.97, 147.26, 139.47, 135.02, 130.52, 130.38, 130.18, 129.72, 129.24, 127.55, 125.42, 119.63, 119.23, 117.47, 113.92, 106.43, 104.03, 42.65, 42.27, 14.41, 13.44.

4.2.4. (Z)-2-((3-(4-bromophenyl)-1-phenyl-1H-pyrazol-4-yl)methylene)-3-oxo-2,3-dihydrobenzofuran-6-yl diethylcarbamate (7d)

Yield: 91 %; Yellow solid; mp: 224–226 °C; IR (KBr) ν (cm^{-1}): 1720 and 1643 (C=O), 1597 (C=C), 1520 (C=N); ^{1}H NMR (400 MHz, $CDCl_3$) δ (ppm): 8.74 (s, 1H, pyrazole), 7.87 (d, J = 8.0 Hz, 2H, Ar), 7.80 (d, J = 8.0 Hz, 1H, Ar), 7.67 (d, J = 8.0 Hz, 2H, Ar), 7.63 (d, J = 8.0 Hz, 2H, Ar), 7.55 (t, J = 7.6 Hz, 2H, Ar), 7.40 (t, J = 7.6 Hz, 1H, Ar), 7.34 (s, 1H, Ar), 6.99–7.00 (m, 2H, Ar, =CH), 3.47 (q, J = 7.2 Hz, 4H, CH_2), 1.33–1.29 (m, 6H, CH_3); ^{13}C NMR (100 MHz, $CDCl_3$) δ (ppm): 182.30, 166.08, 158.41, 153.39, 152.87, 147.21, 139.42, 132.10, 130.91, 130.36, 130.30, 129.62, 127.47, 125.34, 123.20, 119.57, 119.15, 117.36, 113.83, 106.30, 103.88, 42.57, 42.18, 14.31, 13.33.

4.2.5. (Z)-2-((1-phenyl-3-(p-tolyl)-1H-pyrazol-4-yl)methylene)-3-oxo-2,3-dihydrobenzofuran-6-yl diethylcarbamate (7e)

Yield: 94 %; Yellow solid; mp: 195–197 °C; IR (KBr) ν (cm^{-1}): 1720 and 1643 (C=O), 1597 (C=C), 1528 (C=N); ^{1}H NMR (400 MHz, $CDCl_3$) δ (ppm): 8.70 (s, 1H, pyrazole), 7.78 (d, J = 8.4Hz, 1H, Ar), 7.75–7.71 (m, 4H, Ar), 7.52–7.50 (m, 2H, Ar), 7.48–7.46 (m, 1H, Ar), 7.32–7.30 (m, 3H, Ar), 7.06 (s, 1H, =CH), 6.97 (dd, J = 2.0 Hz, J = 8.4 Hz, 1H, Ar), 3.50–3.41 (m, 4H, CH_2), 2.43 (s, 3H, CH_3), 1.42–1.29 (m, 6H, CH_3); ^{13}C NMR (125 MHz, $CDCl_3$) δ (ppm): 182.46, 166.09, 158.37, 154.62, 153.02, 147.08, 137.36, 137.35, 132.06, 130.18, 129.02, 129.00, 128.86, 125.37, 119.55, 119.54, 119.39, 117.37, 113.74, 106.42, 104.92, 42.64, 42.26, 21.17, 14.41, 13.44.

4.2.6. (Z)-2-((3-(4-methoxyphenyl)-1-phenyl-1H-pyrazol-4-yl)methylene)-3-oxo-2,3-dihydrobenzofuran-6-yl diethylcarbamate (7f)

Yield: 96 %; Yellow solid; mp: 196–198 °C; IR (KBr) ν (cm^{-1}): 1720 and 1643 (C=O), 1597 (C=C), 1528 (C=N); ^{1}H NMR (400 MHz, $CDCl_3$) δ (ppm): 8.73 (s, 1H, pyrazole), 7.87 (d, J = 7.6 Hz, 2H, Ar), 7.80 (d, J = 8.4 Hz, 1H, Ar), 7.68 (d, J = 8.4 Hz, 2H, Ar), 7.54 (t, J = 7.6 Hz, 2H, Ar), 7.38 (t, J = 7.6 Hz, 1H, Ar), 7.34 (d, J = 1.6 Hz, 1H, Ar), 7.08–7.06 (m, 3H, Ar, =CH), 6.99 (dd, J = 1.6 Hz, J = 8.4 Hz, 1H, Ar), 3.91 (s, 3H, OCH_3), 3.47 (q, J = 7.2 Hz, 4H, CH_2), 1.32–1.29 (m, 6H, CH_3); ^{13}C NMR (100 MHz, $CDCl_3$) δ (ppm): 182.31, 166.00, 160.19, 158.29, 154.53, 152.92, 147.01, 139.55, 130.14, 130.12, 129.55, 127.20, 125.26, 124.40, 119.50, 119.30, 117.26, 114.41, 113.74, 106.30, 104.88, 55.42, 42.56, 42.18, 14.30, 13.33.

4.2.7. (Z)-2-((3-(4-nitrophenyl)-1-phenyl-1H-pyrazol-4-yl)methylene)-3-oxo-2,3-dihydrobenzofuran-6-yl diethylcarbamate (7g)

Yield: 90 %; Yellow solid; mp: 249–251 °C; IR (KBr) ν (cm^{-1}): 1720 and 1651 (C=O), 1597 (C=C), 1528 (C=N); ^{1}H NMR (400 MHz, $CDCl_3$) δ (ppm): 8.77 (s, 1H, pyrazole), 8.40 (d, J = 8.0 Hz, 2H, Ar), 7.96 (d, J = 8.4 Hz, 2H, Ar), 7.88 (d, J = 7.6 Hz, 2H, Ar), 7.81 (d, J = 8.4 Hz, 1H, Ar), 7.57 (t, J = 7.2 Hz, 2H, Ar), 7.44 (t, J = 7.2 Hz, 1H, Ar), 7.36 (s, 1H, Ar), 7.02–6.98 (m, 2H, Ar, =CH), 3.48 (q, J = 6.8 Hz, 4H, CH_2), 1.33–1.29 (m, 6H, CH_3); ^{13}C NMR (100 MHz, $CDCl_3$) δ (ppm): 182.29, 166.18, 158.57, 152.83, 151.80, 147.86, 147.50, 139.24, 138.51, 130.60, 129.71, 129.46, 127.83, 125.43, 124.16, 119.65, 118.95, 117.52, 114.24, 106.34, 102.83, 42.59, 42.20, 14.31, 13.32.

4.2.8. (Z)-2-((3-(naphthalen-1-yl)-1-phenyl-1H-pyrazol-4-yl)methylene)-3-oxo-2,3-dihydrobenzofuran-6-yl diethylcarbamate (7h)

Yield: 93 %; Yellow solid; mp: 209–211 °C; IR (KBr) ν (cm^{-1}): 1715 and 1644 (C=O), 1595 (C=C), 1527 (C=N); ^{1}H NMR (400 MHz, $CDCl_3$) δ (ppm): 8.81 (s, 1H, pyrazole), 8.22 (s, 1H, Ar), 8.03–7.98 (m, 2H, Ar), 7.94–7.89 (m, 4H, Ar), 7.82 (d, J = 8.4 Hz, 1H, Ar), 7.59–7.55 (m, 4H, Ar), 7.43–7.40 (m, 1H, Ar), 7.36 (d, J = 1.6 Hz, 1H, Ar), 7.17 (s, 1H, =CH), 7.01 (dd, J = 1.6 Hz, J = 8.4 Hz, 1H, Ar), 3.53–3.43 (m, 4H, CH_2), 1.42–1.30 (m, 6H, CH_3); ^{13}C NMR (100 MHz, $CDCl_3$) δ (ppm): 182.26, 166.05, 158.30, 154.59, 152.91, 147.19, 139.56, 133.37, 133.35, 130.33, 129.61, 129.38, 128.67, 128.54, 128.23, 127.78, 127.37, 126.59, 126.45, 126.41, 125.30, 119.64, 119.27, 117.30, 114.15, 106.31, 104.60, 42.56, 42.18, 14.31, 13.33; HRMS (ESI-MS) m/z calcd. for $[C_{33}H_{27}N_3O_4]^+$ $[M+H]^+$: 530.2080; found: 530.2010.

4.2.9. (Z)-2-((3-(naphthalen-2-yl)-1-phenyl-1H-pyrazol-4-yl)methylene)-3-oxo-2,3-dihydrobenzofuran-6-yl diethylcarbamate (7i)

Yield: 95 %; Yellow solid; mp: 202–204 °C; IR (KBr) ν (cm^{-1}) 1716 and 1643 (C=O), 1592 (C=C), 1525 (C=N); ^{1}H NMR (400 MHz, $CDCl_3$) δ (ppm): 8.78 (m, 1H, pyrazole), 8.20–8.19 (m, 1H, Ar), 8.00–7.96 (m, 2H, Ar), 7.92–7.86 (m, 4H, Ar), 7.79 (d, J = 8.4 Hz, 1H, Ar), 7.57–7.52 (m, 4H, Ar), 7.41–7.37 (m, 1H, Ar), 7.33 (d, J = 2.0 Hz, 1H, Ar), 7.15 (s, 1H, =CH), 6.98 (dd, J = 2.0 Hz, J = 8.4 Hz, 1H, Ar), 3.50–3.41 (m, 4H, CH_2), 1.37–1.27 (m, 6H, CH_3); ^{13}C NMR (100 MHz, $CDCl_3$) δ (ppm): 182.33, 166.06, 158.34, 154.62, 152.91, 147.20, 139.57, 133.39, 133.36, 130.34, 129.61, 129.40, 128.68, 128.55, 128.24, 127.78, 127.37, 126.60, 126.45, 126.42, 125.31, 119.64, 119.28, 117.30, 114.16, 106.31, 104.61, 42.57, 42.19, 14.31, 13.33.

4.2.10. (Z)-2-((3-([1,1′-biphenyl]-4-yl)-1-phenyl-1H-pyrazol-4-yl)methylene)-3-oxo-2,3-dihydrobenzofuran-6-yl diethylcarbamate (7j)

Yield: 95 %; Yellow solid; mp: 231–233 °C; IR(KBr) ν (cm^{-1}): 1728 and 1643 (C=O), 1597 (C=C), 1528 (C=N); ^{1}H NMR (400 MHz, $CDCl_3$) δ (ppm): 8.76 (s, 1H, pyrazole), 7.88 (d, J = 7.6 Hz, 2H, Ar), 7.83–7.74 (m, 5H, Ar), 7.69–7.67 (m, 2H, Ar), 7.56–7.47 (m, 4H, Ar), 7.41–7.37 (m, 2H, Ar), 7.33 (d, J = 1.8 Hz, 1H, Ar), 7.12 (s, 1H, =CH), 6.98 (dd, J = 1.8 Hz, J = 8.4 Hz, 1H, Ar), 3.50–3.41 (m, 4H, CH_2), 1.42–1.29 (m, 6H, CH_3); ^{13}C NMR (100 MHz, $CDCl_3$) δ (ppm): 182.32, 166.07, 158.36, 154.31, 152.90, 147.15, 141.64, 140.66, 139.56, 130.89, 130.24, 129.58, 129.24, 128.86, 127.64, 127.55, 127.32, 127.20, 125.30, 119.57, 119.27, 117.29, 113.98, 106.29, 104.55, 42.57, 42.18, 14.30, 13.32.

4.2.11. (Z)-2-((1-phenyl-3-(thiophen-2-yl)-1H-pyrazol-4-yl)methylene)-3-oxo-2,3-dihydrobenzofuran-6-yl diethylcarbamate (7k)

Yield: 92 %; Yellow solid; mp: 211–213 °C; IR (KBr) ν (cm^{-1}): 1744 and 1631 (C=O), 1600 (C=C), 1509 (C=N); ^{1}H NMR (500 MHz, $CDCl_3$) δ (ppm): 8.68 (s, 1H, pyrazole), 7.83 (d, J = 8.0 Hz, 2H, Ar), 7.78 (d, J = 8.2 Hz, 1H, Ar), 7.52–7.49 (m, 3H, Ar), 7.43 (d, J = 5.0 Hz, 1H, Ar), 7.38–7.35 (m, 1H, Ar), 7.31 (s, 1H, Ar), 7.19–7.17 (m, 2H, Ar, =CH), 6.97 (d, J = 8.2 Hz, 1H, Ar), 3.46–3.42 (m, 4H, CH_2), 1.34–1.25 (m, 6H, CH_3); ^{13}C NMR (125 MHz, $CDCl_3$) δ (ppm): 182.40, 166.14, 158.45, 152.97, 148.60, 147.35, 139.36, 133.67, 130.36, 129.67, 128.02, 127.51, 127.26, 126.81, 125.40, 119.60, 119.26, 117.44, 113.82, 106.43, 103.96, 42.64, 42.26, 14.41, 13.43.

4.2.12. (Z)-3-oxo-2-((3-phenyl-1-(p-tolyl)-1H-pyrazol-4-yl)methylene)-2,3-dihydrobenzofuran-6-yl diethylcarbamate (8a)

Yield: 95 %; Bright yellow solid; mp: 190–192 °C; IR (KBr) ν (cm^{-1}): 1713 and 1643 (C=O), 1597 (C=C), 1528 (C=N); ^{1}H NMR (400 MHz, $CDCl_3$) δ (ppm): 8.73 (s, 1H, pyrazole), 7.81 (d, J = 8.4 Hz, 1H, Ar), 7.77–7.73 (m, 4H, Ar), 7.56–7.52 (m, 2H, Ar), 7.48 (t, J = 7.2 Hz, 1H, Ar), 7.35–7.34 (m, 3H, Ar), 7.09 (s, 1H, =CH), 6.70 (dd, J = 1.6 Hz, J = 8.4 Hz, 1H, Ar), 3.52–3.43 (m, 4H, CH_2), 2.45 (s, 3H, CH_3), 1.37–1.29 (m, 6H, CH_3); ^{13}C NMR (100 MHz, $CDCl_3$) δ (ppm): 182.34, 166.00, 158.27, 154.53, 152.91, 150.04, 147.97, 146.99, 137.27, 131.96, 130.08, 128.90, 128.75, 125.27, 124.91, 119.48, 119.30, 117.25, 113.65, 106.30, 104.81, 42.55, 42.17, 21.07, 14.31, 13.34.

4.2.13. (Z)-2-((3-(4-fluorophenyl)-1-(p-tolyl)-1H-pyrazol-4-yl)methylene)-3-oxo-2,3-dihydrobenzofuran-6-yl diethylcarbamate (8b)

Yield: 89 %; Bright yellow solid; mp: 215–217 °C; IR (KBr) ν (cm^{-1}): 1721 and 1643 (C=O), 1600 (C=C), 1520 (C=N); ^{1}H NMR (500 MHz, $CDCl_3$) δ (ppm): 8.67 (s, 1H, pyrazole), 7.78 (d, J = 8.5 Hz, 1H, Ar), 7.72–7.68 (m, 4H, Ar), 7.32–7.30 (m, 3H, Ar), 7.20 (t, J = 8.5 Hz, 2H, Ar), 6.98–6.96 (m, 2H, Ar, =CH), 3.49–3.41 (m, 4H, CH_2), 2.42 (s, 3H, CH_3), 1.30–1.26 (m, 6H, CH_3); ^{13}C NMR (125 MHz, $CDCl_3$) δ (ppm): 182.45, 166.12, 163.29 (d, J = 248.3 Hz), 158.42, 153.59, 153.00, 147.14, 137.48, 137.27, 130.80, 130.73, 130.21, 125.40, 119.54, 119.31, 117.43, 116.14, 115.96, 113.64, 106.42, 104.47, 42.65, 42.26, 21.17, 14.40, 13.43.

4.2.14. (Z)-2-((3-(4-chlorophenyl)-1-(p-tolyl)-1H-pyrazol-4-yl)methylene)-3-oxo-2,3-dihydrobenzofuran-6-yl diethylcarbamate (8c)

Yield: 96 %; Bright yellow solid; mp: 218–220 °C; IR (KBr) ν (cm^{-1}): 1723 and 1646 (C=O), 1604 (C=C), 1530 (C=N); ^{1}H NMR (500 MHz, $CDCl_3$) δ (ppm): 8.65 (s, 1H, pyrazole), 7.76 (d, J = 8.3 Hz, 1H, Ar), 7.70 (d, J = 8.0 Hz, 2H, Ar), 7.65 (d, J = 8.0 Hz, 2H, Ar), 7.47 (d, J = 8.0 Hz, 2H, Ar), 7.31–7.29 (m, 3H, Ar), 6.96–6.95 (m, 2H, Ar, =CH), 3.47–3.41 (m, 4H, CH_2), 2.42 (s, 3H, CH_3), 1.40–1.28 (m, 6H, CH_3); ^{13}C NMR (125 MHz, $CDCl_3$) δ (ppm): 182.42, 166.11, 158.44, 153.24, 152.99, 147.16, 143.87, 137.53, 137.21, 134.94, 130.59, 130.26, 130.21, 130.18, 129.21, 119.52, 119.26, 117.44, 113.66, 106.43, 104.23, 42.64, 42.26, 21.17, 14.41, 13.43.

4.2.15. (Z)-2-((3-(4-bromophenyl)-1-(p-tolyl)-1H-pyrazol-4-yl)methylene)-3-oxo-2,3-dihydrobenzofuran-6-yl diethylcarbamate (8d)

Yield: 94 %; Bright yellow solid; mp: 207–209 °C; IR (KBr) ν (cm^{-1}): 1720 and 1643 (C=O), 1597 (C=C), 1528 (C=N); ^{1}H NMR (400 MHz, $CDCl_3$) δ (ppm): 8.71 (s, 1H, pyrazole), 7.81 (d, J = 8.4 Hz, 1H, Ar), 7.74 (d, J = 8.4 Hz, 2H, Ar), 7.69–7.62 (m, 4H, Ar), 7.35–7.34 (m, 3H, Ar), 7.01–6.98 (m, 2H, Ar, =CH), 3.52–3.43 (m, 4H, CH_2), 2.46 (s, 3H, CH_3), 1.33–1.29 (m, 6H, CH_3); ^{13}C NMR (100 MHz, $CDCl_3$) δ (ppm): 182.31, 166.06, 158.37, 153.21, 152.89, 147.12, 137.46, 137.18, 132.08, 130.98, 130.37, 130.21, 130.12, 125.32, 123.12, 119.50, 119.19, 117.34, 113.59, 106.31, 104.08, 42.57, 42.18, 21.07, 14.30, 13.32.

4.2.16. (Z)-2-((1,3-di-p-tolyl-1H-pyrazol-4-yl)methylene)-3-oxo-2,3-dihydrobenzofuran-6-yl diethylcarbamate (8e)

Yield: 96 %; Bright yellow solid; mp: 203–205 °C; IR (KBr) ν (cm^{-1}): 1728 and 1643 (C=O), 1605 (C=C), 1528 (C=N); ^{1}H NMR (400 MHz, $CDCl_3$) δ (ppm): 8.71 (s, 1H, pyrazole), 7.81 (d, J = 8.4 Hz, 1H, Ar), 7.76 (d, J = 8.4 Hz, 2H, Ar), 7.63 (d, J = 8.0 Hz, 2H, Ar), 7.35–7.33 (m, 5H, Ar), 7.09 (s, 1H, =CH), 7.00–6.98 (m, 1H, Ar), 3.52–3.43 (m, 4H, CH_2), 2.46 (s, 3H, CH_3), 2.45 (s, 3H, CH_3), 1.36–1.29 (m, 6H, CH_3); ^{13}C NMR (100 MHz, $CDCl_3$) δ (ppm): 182.32, 165.97, 158.23, 154.62, 152.92, 146.92, 138.67, 137.31, 137.17, 136.61, 130.05, 129.58, 129.05, 128.76, 125.24, 119.46, 119.34, 117.22, 113.60, 106.29, 105.03, 42.54, 42.17, 21.38, 21.06, 14.31, 13.33.

4.2.17. (Z)-2-((3-(4-methoxyphenyl)-1-(p-tolyl)-1H-pyrazol-4-yl)methylene)-3-oxo-2,3-dihydrobenzofuran-6-yl diethylcarbamate (8f)

Yield: 97 %; Bright yellow solid; mp: 191–193 °C; IR (KBr) ν (cm^{-1}): 1718 and 1645 (C=O), 1604 (C=C), 1522 (C=N); ^{1}H NMR (500 MHz, $CDCl_3$) δ (ppm): 8.66 (s, 1H, pyrazole), 7.77 (d, J = 8.3 Hz, 1H, Ar), 7.72 (d, J = 8.4 Hz, 2H, Ar), 7.65–7.64 (m, 2H, Ar), 7.30–7.29 (m, 3H, Ar), 7.04–7.03 (m, 3H, Ar, =CH), 6.96 (dd, J = 1.8 Hz, J = 8.3 Hz, 1H, Ar), 3.88 (s, 3H, OCH_3), 3.48–3.40 (m, 4H, CH_2), 2.41 (s, 3H, CH_3), 1.29–1.26 (m, 6H, CH_3); ^{13}C NMR (125 MHz, $CDCl_3$) δ (ppm): 182.40, 166.05, 160.22, 158.33, 154.43, 153.02, 146.99, 137.38, 137.23, 130.23, 130.14, 130.09, 125.31, 124.56, 119.49, 119.43, 117.33, 114.46, 113.57, 106.41, 105.14, 55.49, 42.63, 42.24, 21.14, 14.39, 13.42; HRMS (ESI-MS) m/z calcd. for $[C_{31}H_{29}N_3O_5]^+$ $[M+H]^+$: 524.2185; found: 524.2353.

4.2.18. (Z)-2-((3-(4-nitrophenyl)-1-(p-tolyl)-1H-pyrazol-4-yl)methylene)-3-oxo-2,3-dihydrobenzofuran-6-yl diethylcarbamate (8g)

Yield: 96 %; Bright yellow solid; mp: 252–254 °C; IR (KBr) ν (cm^{-1}): 1713 and 1643 (C=O), 1597 (C=C), 1520 (C=N); ^{1}H NMR (400 MHz, $CDCl_3$) δ (ppm): 8.74 (s, 1H, pyrazole), 8.40 (d, J = 8.8 Hz, 2H, Ar), 7.96 (d, J = 8.8 Hz, 2H, Ar), 7.82 (d, J = 8.4 Hz, 1H, Ar), 7.75 (d, J = 8.4 Hz, 2H, Ar), 7.37–7.35 (m, 3H, Ar), 7.02–6.99 (m, 2H, Ar, =CH), 3.52–3.43 (m, 4H, CH_2), 2.47 (s, 3H, CH_3), 1.33–1.29 (m, 6H, CH_3); ^{13}C NMR (100 MHz, $CDCl_3$) δ (ppm): 182.32, 166.16, 158.52, 152.84, 151.63, 147.81, 147.41, 142.52, 138.60, 137.88, 137.00, 130.51, 130.22, 129.47, 125.43, 124.16, 119.57, 117.49, 114.02, 106.35, 103.02, 42.58, 42.19, 21.10, 14.31, 13.33; HRMS (ESI-MS) *m/z* calcd. for $[C_{30}H_{26}N_4O_6]^+$ $[M+H]^+$: 539.1930; found: 539.2106.

4.2.19. (Z)-2-((3-(naphthalen-1-yl)-1-(p-tolyl)-1H-pyrazol-4-yl)methylene)-3-oxo-2,3-dihydrobenzofuran-6-yl diethylcarbamate (8h)

Yield: 92 %; Bright yellow solid; mp: 185–187 °C; IR (KBr) ν (cm^{-1}): 1713 and 1645 (C=O), 1595 (C=C), 1529 (C=N); ^{1}H NMR (500 MHz, $CDCl_3$) δ (ppm): 8.73 (s, 1H, pyrazole), 8.19 (s, 1H, Ar), 7.99–7.90 (m, 4H, Ar), 7.86 (d, J = 8.5 Hz, 1H, Ar), 7.77 (t, J = 8.0 Hz, 3H, Ar), 7.55–7.53 (m, 2H, Ar), 7.33–7.32 (m, 2H, Ar), 7.14 (s, 1H, =CH), 6.98–6.96 (m, 1H, Ar), 3.49–3.41 (m, 4H, CH_2), 2.43 (s, 3H, CH_3), 1.30–1.26 (m, 6H, CH_3); ^{13}C NMR (125 MHz, $CDCl_3$) δ (ppm): 182.44, 166.11, 158.38, 154.51, 153.02, 147.18, 137.43, 137.38, 133.48, 133.41, 130.33, 130.21, 129.55, 128.76, 128.64, 128.31, 127.87, 126.66, 126.56, 126.52, 125.38, 119.62, 119.40, 117.39, 113.99, 106.42, 104.89, 42.64, 42.25, 21.19, 14.41, 13.44.

4.2.20. (Z)-2-((3-(naphthalen-2-yl)-1-(p-tolyl)-1H-pyrazol-4-yl)methylene)-3-oxo-2,3-dihydrobenzofuran-6-yl diethylcarbamate (8i)

Yield: 96 %; Bright yellow solid; mp: 200–202 °C; IR (KBr) ν (cm^{-1}): 1713 and 1646 (C=O), 1599 (C=C), 1526 (C=N); ^{1}H NMR (500 MHz, $CDCl_3$) δ (ppm): 8.73 (s, 1H, pyrazole), 8.18 (s, 1H, Ar), 7.99–7.89 (m, 4H, Ar), 7.87–7.85 (m, 1H, Ar), 7.77 (t, J = 8.0 Hz, 3H, Ar), 7.55–7.53 (m, 2H, Ar), 7.33–7.32 (m, 2H, Ar), 7.14 (s, 1H, =CH), 6.97 (dd, J = 2.0 Hz, J = 8.5 Hz, 1H, Ar), 3.48–3.41 (m, 4H, CH_2), 2.43 (s, 3H, CH_3), 1.30–1.26 (m, 6H, CH_3); ^{13}C NMR (125 MHz, $CDCl_3$) δ (ppm): 182.44, 166.10, 158.37, 154.50, 153.02, 147.17, 137.42, 137.38, 133.47, 133.41, 130.33, 130.21, 129.55, 128.75, 128.64, 128.30, 127.87, 126.65, 126.55, 126.52, 125.37, 119.61, 119.40, 117.38, 113.99, 106.44, 104.88, 42.65, 42.26, 21.18, 14.41, 13.44.

4.2.21. (Z)-2-((3-([1,1′-biphenyl]-4-yl)-1-(p-tolyl)-1H-pyrazol-4-yl)methylene)-3-oxo-2,3-dihydrobenzofuran-6-yl diethylcarbamate (8j)

Yield: 97 %; Bright yellow solid; mp: 225–227 °C; IR (KBr) ν (cm^{-1}): 1730 and 1642 (C=O), 1599 (C=C), 1507 (C=N); ^{1}H NMR (400 MHz, $CDCl_3$) δ (ppm): 8.74 (s, 1H, pyrazole), 7.85–7.81 (m, 3H, Ar), 7.79–7.76 (m, 4H, Ar), 7.70 (d, J = 7.3 Hz, 2H, Ar), 7.51 (t, J = 7.2 Hz, 2H, Ar), 7.41 (t, J = 7.2 Hz, 1H, Ar), 7.36–7.34 (m, 3H, Ar), 7.14 (s, 1H, =CH), 7.00 (dd, J = 1.8 Hz, J = 8.3 Hz, 1H, Ar), 3.52–3.44 (m, 4H, CH_2), 2.46 (s, 3H, CH_3), 1.33–1.30 (m, 6H, CH_3); ^{13}C NMR (100 MHz, $CDCl_3$) δ (ppm): 182.34, 166.03, 158.31, 154.13, 152.91, 147.05, 141.57, 141.17, 140.69, 137.29, 130.96, 130.14, 130.09, 129.25, 128.86, 127.64, 127.53, 127.21, 125.29, 119.49, 119.31, 117.27, 113.74, 106.30, 104.75, 42.56, 42.17, 21.07, 14.31, 13.34.

4.2.22. (Z)-3-oxo-2-((3-(thiophen-2-yl)-1-(p-tolyl)-1H-pyrazol-4-yl)methylene)-2,3-dihydrobenzofuran-6-yl diethylcarbamate (8k)

Yield: 93 %; Brown solid; mp: 143–145 °C; IR (KBr) ν (cm^{-1}): 1718 and 1645 (C=O), 1601 (C=C), 1527 (C=N); ^{1}H NMR (400 MHz, $CDCl_3$) δ (ppm): 8.68 (s, 1H, pyrazole), 7.82 (d, J = 8.4 Hz, 1H, Ar), 7.74 (d, J = 8.4 Hz, 2H, Ar), 7.52–7.51 (m, 1H, Ar), 7.46–7.45 (m, 1H, Ar), 7.34–7.32 (m, 3H, Ar), 7.21–7.20 (m, 2H, Ar, =CH), 7.00 (dd, J = 2.0 Hz, J = 8.4 Hz, 1H, Ar), 3.52–3.43 (m, 4H, CH_2), 2.45 (s, 3H, CH_3), 1.29–1.26 (m, 6H, CH_3); ^{13}C NMR (100 MHz, $CDCl_3$) δ (ppm): 182.30, 166.05, 158.34, 152.89, 148.35, 147.19, 137.39, 137.09, 133.66, 130.17, 130.08, 127.89, 127.11, 126.64, 125.30, 119.47, 119.24, 117.30, 113.54, 106.29, 104.05, 42.56, 42.18, 21.06, 14.30, 13.32.

4.2.23. (Z)-2-((1-(4-nitrophenyl)-3-phenyl-1H-pyrazol-4-yl)methylene)-3-oxo-2,3-dihydrobenzofuran-6-yl diethylcarbamate (9a)

Yield: 92 %; Brown solid; mp: 274–276 °C; IR (KBr) ν (cm^{-1}): 1713 and 1643 (C=O), 1589 (C=C), 1512 (C=N); ^{1}H NMR (400 MHz, $CDCl_3$) δ (ppm): 8.85 (s, 1H, pyrazole), 0.8.43 (d, J = 8.8 Hz, 2H, Ar), 8.09 (d, J = 9.2 Hz, 2H, Ar), 7.82 (d, J = 8.4 Hz, 1H, Ar), 7.74 (d, J = 6.8 Hz, 2H, Ar), 7.59–7.53 (m, 3H, Ar), 7.40 (s, 1H, Ar), 7.03–7.01 (m, 2H, Ar, =CH), 3.49 (q, J = 7.6 Hz, 4H, CH_2), 1.34–1.30 (m, 6H, CH_3); ^{13}C NMR (100 MHz, $CDCl_3$) δ (ppm): 182.26, 166.15, 158.56, 155.88, 152.83, 150.71, 147.70, 145.96, 143.73, 131.20, 130.05, 129.33, 129.05, 128.83, 125.47, 119.03, 118.98, 117.49, 115.55, 106.33, 103.21, 42.61, 42.21, 14.32, 13.33.

4.2.24. (Z)-2-((3-(4-fluorophenyl)-1-(4-nitrophenyl)-1H-pyrazol-4-yl)methylene)-3-oxo-2,3-dihydrobenzofuran-6-yl diethylcarbamate (9b)

Yield: 88 %; Dark brown solid; mp: 283–285 °C; IR (KBr) ν (cm^{-1}): 1712 and 1643 (C=O), 1599 (C=C), 1519 (C=N); ^{1}H NMR (400 MHz, $CDCl_3$) δ (ppm): 8.84 (s, 1H, pyrazole), 8.43 (d, J = 9.2 Hz, 2H, Ar), 8.08 (d, J = 8.8 Hz, 2H, Ar), 7.82 (d, J = 8.4 Hz, 1H, Ar), 7.75–7.72 (m, 2H, Ar), 7.40 (d, J = 1.6 Hz, 1H, Ar), 7.25 (d, J = 8.4 Hz, 2H, Ar), 7.02 (dd, J = 1.6 Hz, J = 8.4 Hz, 1H, Ar), 6.96 (s, 1H, =CH), 3.48 (q, J = 7.6 Hz, 4H, CH_2), 1.34–1.30 (m, 6H, CH_3); HRMS (ESI-MS) *m/z* calcd. for $[C_{29}H_{23}FN_4O_6]^+$ $[M+H]^+$: 543.1680; found: 543.1863.

4.2.25. (Z)-2-((3-(4-chlorophenyl)-1-(4-nitrophenyl)-1H-pyrazol-4-yl)methylene)-3-oxo-2,3-dihydrobenzofuran-6-yl diethylcarbamate (9c)

Yield: 93 %; Brown solid; mp: 301–303 °C; IR (KBr) ν (cm^{-1}): 1705 and 1651 (C=O), 1597 (C=C), 1504 (C=N); ^{1}H NMR (500 MHz, $CDCl_3$) δ (ppm): 9.12–9.11 (m, 1H, pyrazole), 8.73–8.70 (m, 1H, Ar), 8.38–8.36 (m, 1H, Ar), 8.12–8.09 (m, 1H, Ar), 7.99–7.96 (m, 2H, Ar), 7.84–7.81 (m, 2H, Ar), 7.68–7.67 (m, 1H, Ar), 7.57–7.56 (m, 2H, Ar), 7.31–7.28 (m, 1H, Ar), 7.24–7.23 (m, 1H, =CH), 3.80–3.73 (m, 4H, CH_2), 1.20–1.16 (m, 6H, CH_3); ^{13}C NMR (100 MHz, $CDCl_3$) δ (ppm): 182.22, 166.19, 158.62, 154.59, 152.81, 147.80, 146.07,

143.60, 135.55, 130.14, 130.05, 129.72, 129.32, 125.52, 125.50, 119.07, 118.89, 117.56, 115.47, 106.34, 102.59, 42.62, 42.21, 14.31, 13.32.

4.2.26. (Z)-2-((3-(4-bromophenyl)-1-(4-nitrophenyl)-1H-pyrazol-4-yl)methylene)-3-oxo-2,3-dihydrobenzofuran-6-yl diethylcarbamate (9d)

Yield: 90 %; Brown solid; mp: 310–312 °C; IR (KBr) ν (cm^{-1}): 1705 and 1651 (C=O), 1597 (C=C), 1512 (C=N); ^{1}H NMR (500 MHz, $CDCl_3$) δ (ppm): 8.82 (s, 1H, pyrazole), 8.42–8.41 (m, 2H, Ar), 8.07–8.05 (m, 2H, Ar), 7.80 (d, J = 8.3 Hz, 1H, Ar), 7.70–7.68 (m, 2H, Ar), 7.62–7.60 (m, 2H, Ar), 7.38 (d, J = 1.8 Hz, 1H, Ar), 7.00 (dd, J = 1.8 Hz, J = 8.3 Hz, 1H, Ar), 6.93 (s, 1H, =CH), 3.49–3.43 (m, 4H, CH_2), 1.32–1.29 (m, 6H, CH_3); ^{13}C NMR (100 MHz, $CDCl_3$) δ (ppm): 187.67, 166.19, 158.63, 154.62, 152.81, 147.81, 146.08, 143.60, 132.27, 131.29, 130.31, 130.18, 130.15, 125.52, 125.50, 119.08, 118.88, 117.57, 115.45, 106.35, 102.55, 42.62, 42.22, 14.31, 13.32.

4.2.27. (Z)-2-((1-(4-nitrophenyl)-3-(p-tolyl)-1H-pyrazol-4-yl)methylene)-3-oxo-2,3-dihydrobenzofuran-6-yl diethylcarbamate (9e)

Yield: 95 %; Yellow solid; mp: 309–311 °C; IR (KBr) ν (cm^{-1}): 1705 and 1651 (C=O), 1597 (C=C), 1512 (C=N); ^{1}H NMR (500 MHz, $CDCl_3$) δ (ppm): 8.81 (s, 1H, pyrazole), 8.41–8.39 (m, 2H, Ar), 8.07–8.05 (m, 2H, Ar), 7.79 (d, J = 8.3 Hz, 1H, Ar), 7.61 (d, J = 8.0 Hz, 2H, Ar), 7.36 (d, J = 1.8 Hz, 1H, Ar), 7.35 (d, J = 7.8 Hz, 2H, Ar), 7.00 (s, 1H, =CH), 6.98 (dd, J = 1.8 Hz, J = 8.3 Hz, 1H, Ar), 3.50–3.42 (m, 4H, CH_2), 2.45 (s, 3H, CH_3), 1.31–1.26 (m, 6H, CH_3); ^{13}C NMR (100 MHz, $CDCl_3$) δ (ppm): 182.25, 166.13, 158.52, 155.97, 152.84, 147.64, 145.88, 143.76, 139.39, 129.99, 129.74, 128.70, 128.28, 125.46, 125.44, 119.02, 118.97, 117.46, 115.52, 106.33, 103.43, 42.61, 42.21, 21.42, 14.32, 13.32.

4.2.28. (Z)-2-((3-(4-methoxyphenyl)-1-(4-nitrophenyl)-1H-pyrazol-4-yl)methylene)-3-oxo-2,3-dihydrobenzofuran-6-yl diethylcarbamate (9f)

Yield: 94 %; Yellow solid; mp: 260–262 °C; IR (KBr) ν (cm^{-1}): 1713 and 1644 (C=O), 1598 (C=C), 1520 (C=N); ^{1}H NMR (400 MHz, $CDCl_3$) δ (ppm): 9.04 (s, 1H, pyrazole), 7.88 (d, J = 8.4 Hz, 2H, Ar), 7.77–7.75 (m, 2H, Ar), 7.61–7.58 (m, 2H, Ar), 7.34 (d, J = 8.4 Hz, 2H, Ar), 7.12–7.10 (m, 2H, Ar), 7.04 (dd, J = 2.0 Hz, J = 8.4 Hz, 1H, Ar), 6.74 (s, 1H, =CH), 3.81 (s, 3H, OCH_3), 3.43–3.39 (m, 4H, CH_2), 1.20–1.17 (m, 6H, CH_3).

4.2.29. (Z)-2-((1,3-bis(4-nitrophenyl)-1H-pyrazol-4-yl)methylene)-3-oxo-2,3-dihydrobenzofuran-6-yl diethylcarbamate (9g)

Yield: 96 %; Brown solid; mp: 227–229 °C; IR (KBr) ν (cm^{-1}): 1720 and 1659 (C=O), 1597 (C=C), 1512 (C=N); ^{1}H NMR (400 MHz, $CDCl_3$) δ (ppm): 8.88 (s, 1H, pyrazole), 8.48–8.43 (m, 4H, Ar), 8.11 (d, J = 9.2 Hz, 2H, Ar), 7.97 (d, J = 8.8 Hz, 2H, Ar), 7.84 (d, J = 8.4 Hz, 1H, Ar), 7.42 (s, 1H, Ar), 7.05–7.02 (m, 1H, Ar), 6.95 (s, 1H, =CH), 3.49 (q, J = 7.6 Hz, 4H, CH_2), 1.34–1.32 (m, 6H, CH_3); ^{13}C NMR (125 MHz, $CDCl_3$) δ (ppm): 182.52, 168.14, 157.47, 153.15, 148.25, 148.15, 137.79, 130.57, 129.66, 129.08, 129.07, 125.74, 125.66, 125.60, 124.37, 119.36, 117.82, 115.82, 114.60, 106.50, 104.16, 42.72, 42.03, 14.25, 13.42.

4.2.30. (Z)-2-((3-(naphthalen-1-yl)-1-(4-nitrophenyl)-1H-pyrazol-4-yl)methylene)-3-oxo-2,3-dihydrobenzofuran-6-yl diethylcarbamate (9h)

Yield: 90 %; Brown solid; mp: 196–198 °C; IR (KBr) ν (cm^{-1}): 1719 and 1645 (C=O), 1598 (C=C), 1526 (C=N); ^{1}H NMR (400 MHz, $CDCl_3$) δ (ppm): 8.96 (s, 1H, pyrazole), 8.46–8.44 (m, 2H, Ar), 8.14–8.12 (m, 2H, Ar), 8.05–8.04 (m, 1H, Ar), 7.99–7.94 (m, 4H, Ar), 7.77 (d, J = 8.3 Hz, 1H, Ar), 7.65–7.63 (m, 2H, Ar), 7.41 (d, J = 1.8 Hz, 1H, Ar), 7.00 (dd, J = 1.8 Hz, J = 8.3 Hz, 1H, Ar), 6.63 (s, 1H, =CH), 3.51–3.46 (m, 4H, CH_2), 1.32–1.30 (m, 6H, CH_3); ^{13}C NMR (100 MHz, $CDCl_3$) δ (ppm): 182.87, 166.61, 159.98, 151.95, 143.77, 142.29, 136.89, 134.77, 133.94, 133.81, 129.98, 129.01, 128.77, 128.52, 128.17, 126.95, 126.35, 125.51, 125.46, 125.43, 125.31, 119.10, 117.59, 115.33, 113.22, 106.29, 103.23, 42.96, 42.22, 14.13, 13.33.

4.2.31. (Z)-2-((3-(naphthalen-2-yl)-1-(4-nitrophenyl)-1H-pyrazol-4-yl)methylene)-3-oxo-2,3-dihydrobenzofuran-6-yl diethylcarbamate (9i)

Yield: 92 %; Brown solid; mp: 274–276 °C; IR (KBr) ν (cm^{-1}): 1711 and 1647 (C=O), 1601 (C=C), 1519 (C=N); ^{1}H NMR (400 MHz, $CDCl_3$) δ (ppm): 8.88 (s, 1H, pyrazole), 8.44 (d, J = 8.8 Hz, 2H, Ar), 8.22 (s, 1H, Ar), 8.12 (d, J = 9.2 Hz, 2H, Ar), 8.03 (d, J = 8.4 Hz, 1H, Ar), 7.96–7.94 (m, 2H, Ar), 7.89–7.86 (m, 1H, Ar), 7.82 (d, J = 8.4 Hz, 1H, Ar), 7.60–6.58 (m, 2H, Ar), 7.41 (d, J = 1.2 Hz, 1H, Ar), 7.12 (s, 1H, =CH), 7.02 (dd, J = 1.2 Hz, J = 8.4 Hz, 1H, Ar), 3.52–3.46 (m, 4H, CH_2), 1.34–1.31 (m, 6H, CH_3); ^{13}C NMR (100 MHz, $CDCl_3$) δ (ppm): 182.05, 166.16, 163.83, 160.16, 158.56, 147.79, 145.98, 143.74, 133.54, 133.31, 130.15, 129.97, 128.87, 128.65, 128.57, 128.39, 127.83, 126.67, 126.08, 125.49, 125.46, 119.07, 117.50, 115.78, 113.70, 106.34, 103.21, 42.60, 42.21, 14.12, 13.32.

4.2.32. (Z)-2-((3-([1,1′-biphenyl]-4-yl)-1-(4-nitrophenyl)-1H-pyrazol-4-yl)methylene)-3-oxo-2,3-dihydrobenzofuran-6-yl diethylcarbamate (9j)

Yield: 93 %; Brown solid; mp: 200–202 °C; IR (KBr) ν (cm^{-1}): 1713 and 1644 (C=O), 1597 (C=C), 1520 (C=N); ^{1}H NMR (400 MHz, $CDCl_3$) δ (ppm): 8.86 (s, 1H, pyrazole), 8.44 (d, J = 9.2 Hz, 2H, Ar), 8.10 (d, J = 9.2 Hz, 2H, Ar), 7.98–7.95 (m, 1H, Ar), 7.82–7.80 (m, 4H, Ar), 7.71–7.69 (m, 2H, Ar), 7.52 (t, J = 7.2 Hz, 3H, Ar), 7.40 (d, J = 1.6 Hz, 1H, Ar), 7.08 (s, 1H, =CH), 7.02 (dd, J = 1.6 Hz, 8.0 Hz, 1H, Ar), 3.54–3.50 (m, 2H, CH_2), 3.48–3.44 (m, 2H, CH_2), 1.34–1.30 (m, 6H, CH_3); ^{13}C NMR (100 MHz, $CDCl_3$) δ (ppm): 182.25, 166.16, 158.57, 147.73, 145.96, 143.71, 142.17, 140.43, 130.10, 129.48, 129.19, 129.04, 128.93, 127.76, 127.38, 127.30, 127.20, 125.48, 119.68, 119.02, 117.50, 115.60, 112.89, 106.35, 103.17, 42.62, 42.22, 14.32, 13.33; HRMS (ESI-MS) m/z calcd. for $[C_{35}H_{28}N_4O_6]^+$ $[M+H]^+$: 601.2087; found: 601.2315.

4.2.33. (Z)-2-((1-(4-nitrophenyl)-3-(thiophen-2-yl)-1H-pyrazol-4-yl)methylene)-3-oxo-2,3-dihydrobenzofuran-6-yl diethylcarbamate (9k)

Yield: 91 %; Yellow solid; mp: 285–287 °C; IR (KBr) ν (cm^{-1}): 1704 and 1645 (C=O), 1593 (C=C), 1513 (C=N); ^{1}H NMR (400 MHz, $CDCl_3$) δ (ppm): 8.81 (s, 1H, pyrazole), 8.44–8.42 (m, 2H, Ar), 8.08–8.06 (m, 2H, Ar), 7.83 (d, J = 8.3 Hz, 1H, Ar), 7.57–7.55 (m, 1H, Ar), 7.52–7.50 (m, 1H, Ar), 7.39 (d, J = 1.8 Hz, 1H, Ar), 7.25–7.23 (m, 1H, Ar), 7.17 (s, 1H, =CH), 7.02 (dd, J = 1.8 Hz, J = 8.3 Hz, 1H, Ar), 3.48 (q, J = 7.2 Hz, 4H, CH_2), 1.36–1.30 (m, 6H, CH_3); ^{13}C NMR (100 MHz, $CDCl_3$) δ (ppm): 182.21, 166.18, 158.60, 152.80, 147.89, 146.02, 143.47, 132.80, 130.15, 128.09, 127.73, 127.38, 125.50, 125.47, 124.75, 119.04, 118.91, 117.54, 115.30, 106.33, 102.50, 42.60, 42.21, 14.32, 13.32.

4.3. Anticancer studies

4.3.1. General

The *in vitro* anticancer or cell inhibition activities were estimated against the gastric adenocarcinoma cell line, AGS. IC_{50} values (μM) of these compounds were determined using MTT method.

4.3.1.1. Cell culture. AGS cells (CRL-1739) were allowed to grow in Ham's F12–K medium supplemented with 10 % fetal bovine serum and 1 % penicillin/streptomycin cocktail in an optimal CO_2 incubator condition having a humidified atmosphere of 95 % air and 5 % CO_2 at 37 ^{0}C. Cell were washed using sterile phosphate buffer saline (PBS), pH 7.4. Cells that reached 70–80 % confluence were used for MTT assay.

4.3.1.2. MTT assay. Cells were trypsinized and counted to get a final concentration of 1 × 10^5 cells/mL and seeded evenly (100 μL/well) in 96 well micro-titer plates in F12–K medium supplemented with 10% FBS. Next, cells were subjected to increasing drug concentrations in triplicates alongside the untreated cells for the compounds and incubated at 37 ^{0}C for 24 h. Thereafter, the cells in each well were treated with 0.020 ml of 3-[4,5-dimethylthiazol-2-yl]-2,5-diphenyltetrazolium bromide (MTT) solution (5 mg/ml dissolved in PBS) for 2 h at 37 ^{0}C. Addition of DMSO dissolved the insoluble formazan crystals formed by MTT. The absorbance was measured at 570 nm in ELISA Reader (Tecan, Austria) using i-control 1.8 SP1 software. The untreated cells were reference negative control and lysis buffer was used as blank to calculate the % cell viability with the formula:

$$\%\ \text{cell viability} = (\text{OD of the experiment samples} / \text{OD of the negative control}) \times 100$$

The IC_{50} was evaluated by plotting triplicate data sets for each drug concentration. Cytotoxicity was expressed as the drug concentration of the compound that reduces the viability of the cells by 50 % (IC_{50}). The IC_{50} value of the cells was calculated using Microsoft Excel.

4.3.2. In-vitro anticancer studies

The *in vitro* study indicates that many of these newly synthesized carbamates of pyrazole-based 6-hydroxyaurones possess significant anti-proliferative activity. The IC_{50} values of all the tested compounds are summarized in Table 1. Among these aurone analogs **7(e,f)**, **8a**, **8c**, **8(d–f),** and **8(i–k)** exhibited some highly potential cytotoxic activities whereas compounds **9g** (IC_{50} = 74.7 μM), and **9h** (IC_{50} = 71.6 μM) shows very weak anti-proliferative/cytotoxic activities in comparison to the standard reference drugs, Oxaliplatin (IC_{50} = 29.8 μM) and Leucovorin ((IC_{50} = 30.8 μM) against AGS cell line. Among the compounds, **8e** (IC_{50} = 6.5 μM), **8f** (IC_{50} = 6.6 μM), and **7e** (IC_{50} = 10.3 μM) displayed remarkable results as significantly inhibited cell proliferation even better than the reference drugs. Compound **8e** was found to have IC_{50} = 6.5 μM and thus emerged as the most promising cytotoxic agent among this library of compounds. Cancer cells treated with **8e** showed some significant morphological changes at different concentrations compared to the untreated cells (Fig. 4). Most of the cells became smaller, and round and lost their elongated or dendritic projection [76,94].

Table 2
Molecular interaction profile of **7(a-k)**compounds with HER2 kinase domain.

Ligands	Docking energy (K.cal/mol)	*Interacting residues
7a	−110.30	LEU852, VAL734, ALA751, LEU796, CYS805, GLY729, GLY804, LYS753, THR862
7b	−114.38	**MET801**, LEU852, ALA751, LYS753, THR862, LEU796, VAL734, GLY729, CYS805
7c	−111.83	LEU852, MET801, ALA751, LEU800, THR762, LYS753, LEU796, VAL734, CYS805, GLY729
7d	−112.40	LEU852, MET801, ALA751, LEU800, ASP863, THR862, LEU796, VAL734, GLY729, CYS805, LYS753
7e	−121.91	**MET801**, **LYS753,** CYS805, LEU726, LEU785, LEU796, ASP863, LEU852, VAL734, ALA751
7f	−118.15	**MET801**, GLY804, LEU726, LEU852, VAL734, ALA751, LYS753, LEU796, SER728, LEU800
7g	−117.05	**MET801**, ASP863, LYS753, LEU726, LEU852, THR798, ALA751, LEU796, VAL734, LEU785, GLY729,
7h	−108.73	LYS724, CYS805, LEU852, GLY804, LEU726, LEU800, MET801, ALA751, ALA730, ARG849
7i	−110.65	CYS805, VAL734, LEU726, LEU852, LEU800, ALA751, LYS753, MET801, LEU796
7j	−113.12	CYS805, VAL734, SER728, LEU726, LEU852, ASP863, ALA751, LYS753, ASP808, THR862
7k	−116.32	**MET801**, ASP808, LEU726, LEU852, CYS805, THR862, LEU785, LEU796, LYS753, ALA751, VAL734

*Molecular interaction profile of compounds with the H-bond forming residues highlighted in green colour..

4.4. Molecular docking

Docking simulations for the assessment of binding affinities and molecular interactions were done for the synthesized compounds. It was done through the iGEMDOCK version2.1 software (http://gemdock.life.nctu.edu.tw/dock/). **GEMDOCK** stands for **G**enetic **E**volutionary **M**ethod for molecular **D**ocking [95]. iGEMDOCK is a graphical automatic drug design system for docking, screening and analysis. *In-silico* docking simulation studies were performed to evaluate the molecular interactions of three series of 33 compounds, **7(a–k)**, **8(a–k)** and **9(a–k)** (Tables 2, 3 and 4) with the Human Epidermal Growth Factor Receptor kinase domain, HER2 (PDB: 3PP0) protein with a co-crystallized ligand (**SYR127063**) [96]. The 2D structure of the ligands was drawn through BIOVIA Draw software and saved in mol format. The ligand structures were optimized and minimized through Avogadro software. The macromoleculewas cleaned from water residues and protein preparation done with Maestro [97]. The ligand interactions were visualized and analysed through Discovery Visualizer (Biovia).

The scoring function estimates fitness by combining van der Waal energy, hydrogen bonding energy and electro statistic energy. The scoring function includes the following parameters of intermolecular and intramolecular energies and penalty if the ligand is out of range of the search box $E_{tot} = E_{inter} + E_{intra} + E_{penal.}$

In the present docking study HER2 was chosen as the target to explore the molecular interactions due to the evaluation of *in-vitro* activity with these compounds on the gastro cell line and also having understand the role of HER2 in the pathology of gastric cancer [98]. The inhibition of HER2 with novel compounds could yield promising anti-cancer agents. Top one compound from each series with better binding energy and molecular interaction profile was chosen for post docking analysis of interactions (Figs 5, 6, 7, 8, 9 and 10).

4.4.1. Compound 7e interactions with HER2

Compound **7e** exhibits two hydrogen bonding interactions with the active site residues (Table 2) . The two –C=O functionalities on the aurone ring and carbamate were displaying H-bonds with MET801 (3.43 Å) and LYS753 (3.22 Å) amino acids. It has alkyl and π-alkyl interactions with LEU726, VAL734, ALA751, LEU852, LEU796, LEU785 and CYS805 residues. It also shows van der Waals interactions with LEU800, ASN850, GLY729, THR862, THR798, PHE864, ASP808, GLY804, GLY727 and SER728 amino acids in the binding site (Fig. 5).

4.4.2. Compound 8e interactions with HER2

Compound 8e is also displaying two hydrogen bonds with the similar active site residues like 7e (Table 3). The two –C=O groups on the aurone ring and carbamate were displaying H-bonds with MET801 (3.24 Å) and LYS753 (3.13 Å) amino acids. ASP863, ALA751, VAL734, LEU852, LEU726 were involved in the pi-alkyl interactions with the aromatic rings of the scaffold and then LEU785, LEU796 are showing alkyl interactions diethyl carbamate moiety and the remaining residues like GLN799, ASN850, LEU800, GLY729, SER728, CYS805, GLY727, GLY804, ASP808, PHE864, THR798 and THR862 had Vander Waal's interactions with the compound(Fig. 6).

4.4.3. Compound 9c interactions with HER2

9c is also displaying two hydrogen bonds with the similar active site residues like **7e** and **8e (**Table 4**)**. The two –C=O functional groups on the aurone ring and carbamate were displaying H-bonds with MET801 (3.29 Å) and LYS753 (3.24 Å) amino acids. The other major contributor for the binding energy is from the pi-alkyl interactions of aromatic rings of the scaffold and ALA751, LEU852, VAL734 and LEU726 active site residues and then a similar alkyl interaction of LEU785, LEU796 residues with diethyl carbamate moiety were observed and the remaining amino acid residues of binding site had Vander Waal's interactions with the compound (Fig. 7).

The similar binding modes of compounds in the active site can be viewed from their pocket surface images (Fig. 8).The C=O groups present in the aurone ring and carbamate groups in all the compounds are presented in deeply seated orientations and displaying similar interactions with the amino acid residues MET801 and LYS753. MET801 residue had a specific H-bond interaction with aurone ring carbonyl group whereas the carbamate carbonyl group interacting with LYS753 in the active site.

Table 3
Molecular interaction profile of **8(a–k)** compounds with HER2 kinase domain.

Ligands	Docking energy (K.cal/mol)	*Interacting residues
8a	−111.85	MET801, LYS753, LEU726, LEU796, LEU785, ASP863, LEU852, ALA751, VAL734
8b	−110.59	CYS805, LEU800, LEU726, VAL734, GLY729, ASP863, ARG849, ALA730
8c	−117.72	LEU852, MET801, ALA751, LEU800, LYS753, LEU785, PHE864, MET774, GLY727, CYS805, VAL734, THR862
8d	−114.96	PHE864, MET774, LEU785, ASP863, LYS753, LEU800, ALA751, MET801, LEU852, VAL734, CYS805
8e	−124.85	**MET801**, **LYS753**, LEU785, LEU796, ASP863, ALA751, VAL734, LEU852, LEU726
8f	−114.50	CYS805, ALA751, ASP863, THR862, LYS753, MET774, LEU785, VAL734, GLY727, LEU852
8g	−120.49	**MET801**, ALA751, GLY804, LEU785, MET774, LEU796, LYS753, VAL734, GLY727, CYS805, ASP863
8h	−113.12	CYS805, LYS724, LEU852, LEU726, LEU800, MET801, ALA751, ARG849, ALA730
8i	−112.23	**MET801**, LEU726, LEU852, VAL734, ASP808, ALA751
8j	−109.25	CYS805, SER728, ASP808, LEU785, LYS753, ALA751, ASP863, VAL734, LEU852, LEU726
8k	−114.72	**MET801**, LEU726, LEU852, LEU796, LEU785, LYS753, THR862, ALA751, VAL734

*Molecular interaction profile of compounds with the H-bond forming residues highlighted in green colour.

Table 4
Molecular interaction profile of **9(a-k)**compounds with HER2 kinase domain.

Ligands	Docking energy (K.cal/mol)	*Interacting residues
9a	−102.12	CYS805, LEU726, GLY804, ALA751, LEU852, VAL734, LYS753
9b	−109.04	**MET801**, LEU852, ALA751, VAL734, ASP863, CYS805, LEU785, LYS753
9c	−120.46	**MET801**, **LYS753**, LEU726, LEU852, ALA751, ASP863, VAL734, LEU785, LEU796
9d	−106.28	MET801, LEU800, LEU800, LEU852, ALA751, GLY727, CYS805, ASP808, VAL734, GLY729
9e	−116.36	**MET801,** GLU770, GLY804, LEU800, LEU726, LEU852, ALA751, VAL734, LYS753
9f	−112.78	**CYS805**, LYS724, LYS736, LEU726, VAL734, ASP863, ARG849, GLY729, PRO802
9g	−116.33	**MET801**, ASP808, ASP863, LYS753, LEU785, LEU796, LEU852, LEU726, LEU800, ALA751
9h	−111.59	ASP863, ARG849, LYS753, VAL734, SER728, CYS805, LEU726, PRO802
9i	−110.24	**MET801**, ASP808, LEU726, ALA751, VAL734, LEU852
9j	−119.26	**ASP863**, **CYS805**, THR862, LEU726, MET801, ALA751, LEU852, LEU800, LEU796, GLU770
9k	−115.82	**MET801**, GLY804, GLU770, LYS753, VAL734, LEU852, LEU880, LEU726, ALA751

*Molecular interaction profile of compounds with the H-bond forming residues highlighted in green colour.

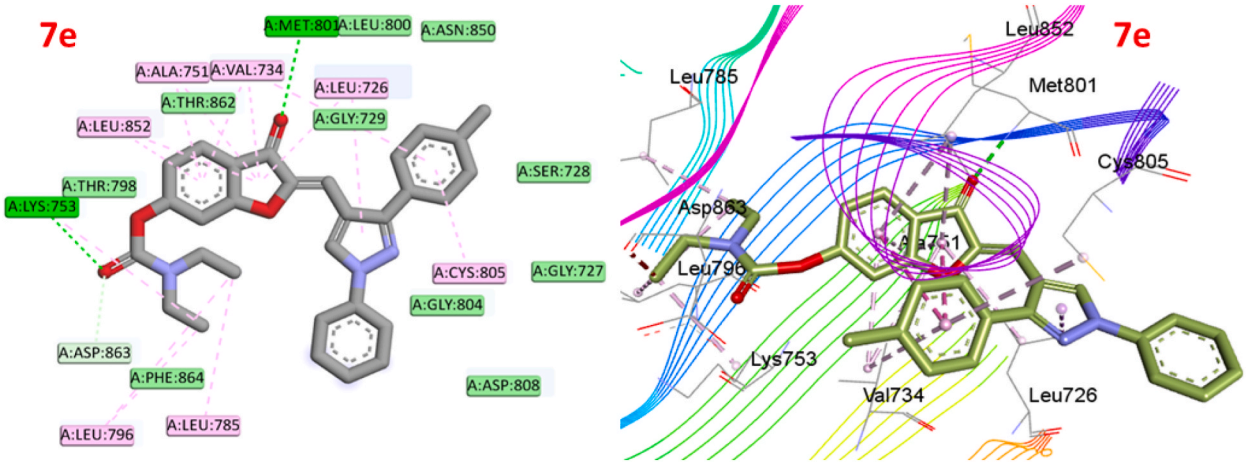

Fig. 5. 2D plot of 7e HER2 interactions (Left side) 3D graphical image with H-bonds denoted as dashed green lines (right side).

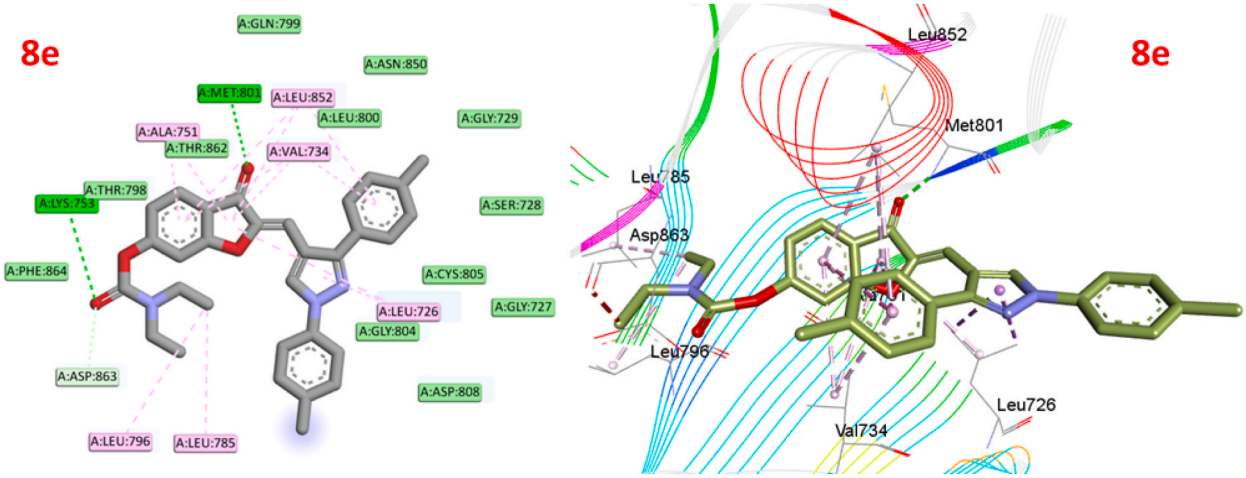

Fig. 6. 2D plot of **8e**HER2 interactions (left side),3D graphical image with H-bonds denoted as dashed green lines (right side)

The comparison of molecular interactions and binding poses of all the docked compounds with the co-crystallized ligand indicates that these compounds had comparable and similar H-bonds (MET801), pi-sigma (LEU852, LEU726), pi-alkyl (LEU785, VAL734, LYS753) interactions and pi-pi stacked interaction with PHE864 active site residues in the binding pocket (Figs. 9 and 10).

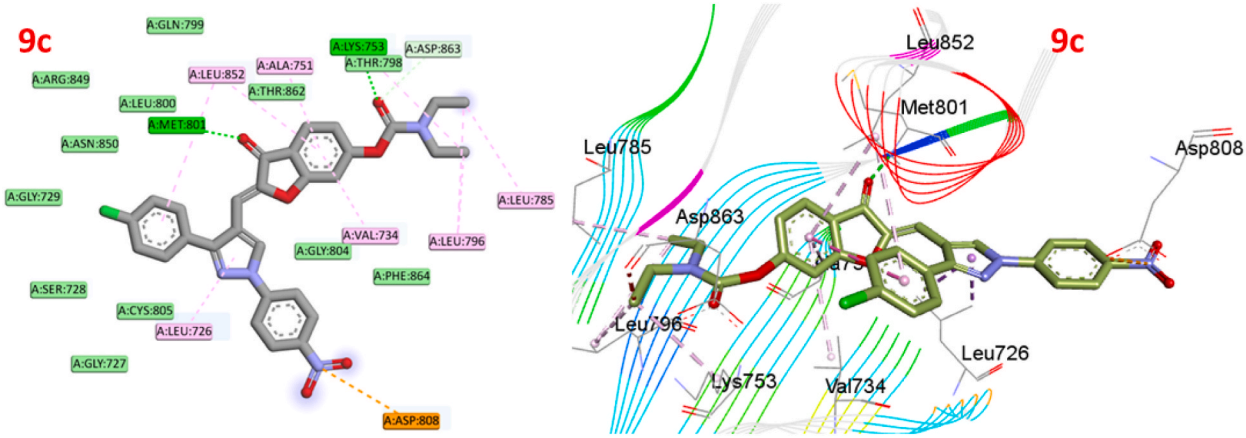

Fig. 7. 2D plot of 9c HER2 interactions (left side),3D graphical image with H-bonds denoted as dashed green lines (right side)

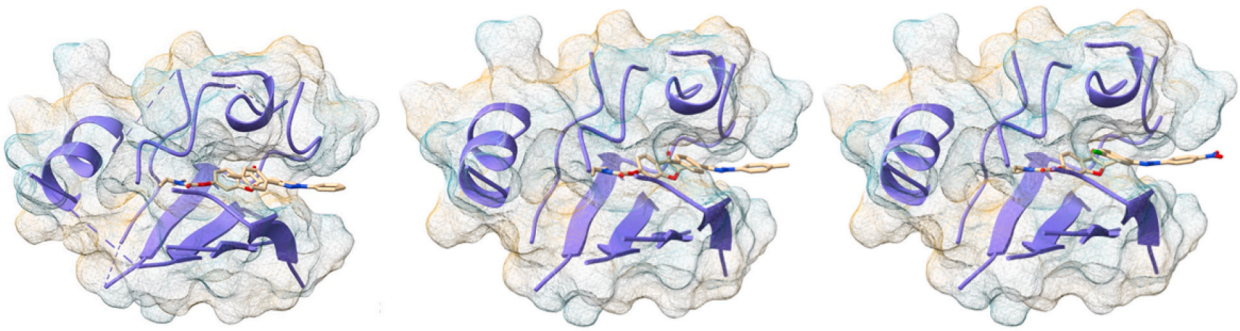

Fig. 8. Active site pocket surface and binding modes of **7e**, **8e** and **9c** compounds with the HER2 Protein.

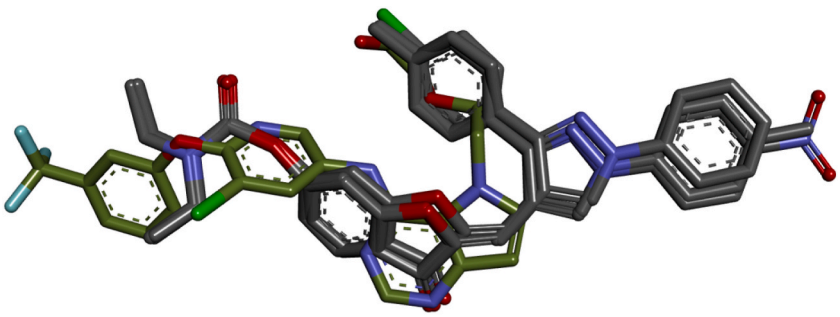

Fig. 9. 7e, **8e**, **9c** and SYR127063 [96](Co-crystallized ligand in gold colour) molecular alignment in theHER2 kinase domain active site pocket

4.5. ADME properties

The potential anti-cancer compounds identified and predicted through the *in vitro* and *in silico* screenings, were assessed for their ADME properties through the SWISS ADME webserver (http://www.swissadme.ch/) [99]. The Lipinkski Drug likeness of the compounds are good with slight deviations in the molecular weight in **8e** and **9c** compounds. No BBB permeation and P-gp substrate activity for these compounds. Regarding the metabolism, CYP2C9 and CYP2C19 isoforms are inhibited by all the compounds whereas CYP3A4 inhibition was predicted for **9c**. Pharmacokinetic properties like GI absorption is low for **9c** compound and further optimization to enhance the pharmaceutical properties could be considered in the future studies(Table 5).

In all the potential compounds carbonyl substituents on the scaffold are mainly involved in the H-bond interactions with the critical amino acid residues in HER2 protein. From the molecular docking studies, it was observed that there is a better co-relation between the *in silico* binding energies and the *in vitro* activity of **7e** and **8e** compounds. These compounds could be further explored as a promising

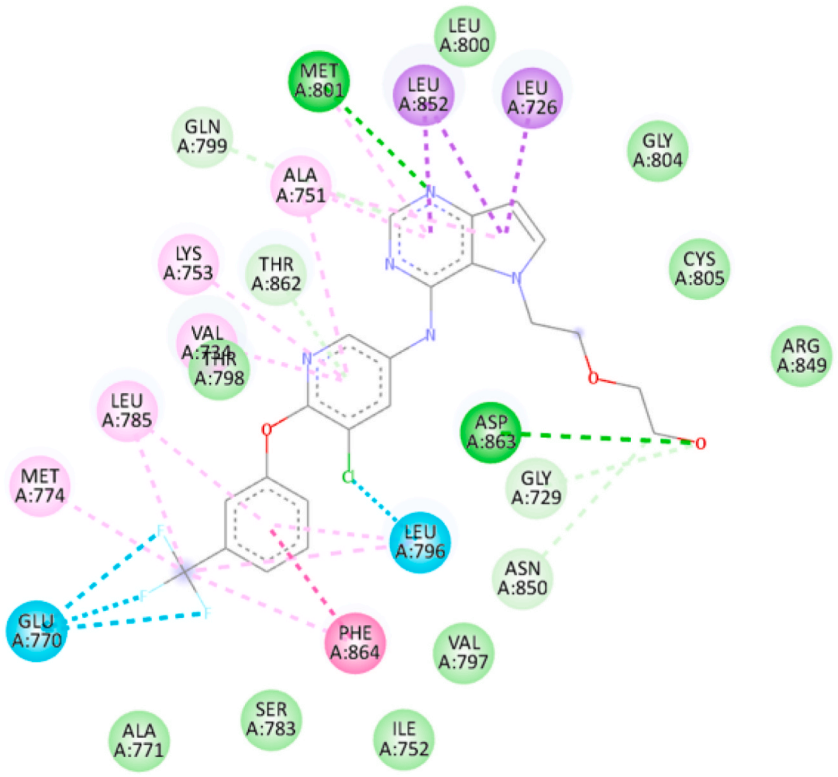

Fig. 10. Molecular interaction profile of SYR127063 [96] (Co-crystallized ligand) with HER2.

Table 5
Physico-chemical properties and drug-likeness prediction of compounds with better *invitro* and *insilico* performance using SWISS ADME [99].

Parameters	7e	8e	9c
Molecular Weight (g/mol)	493.55	507.58	558.97
Log P o/w	5.22	5.55	4.72
No.of. H-bond Donors	0	0	0
No.of H-bond Acceptors	5	5	7
Solubility	Poor	Poor	Poor
TPSA	73.66 Å^2	73.66 Å^2	62.58 Å^2
GI absorption	High	High	Low
BBB permeation	No	No	Yes
P-gp substrate	No	Yes	No
Drug likeness (Lipinski)	Yes	Yes	Yes
Bioavailability score	0.55	0.55	0.55
CYP450 isoforms inhibition	2C9, 2C19	2C9, 2C19	2C9, 2C19, 3A4

lead compound for the anti-cancer activity.

CRediT authorship contribution statement

Ekta Lathwal: Writing – original draft, Methodology, Data curation. **Sanjeev Kumar:** Methodology, Investigation. **Pranab Kumar Sahoo:** Methodology, Investigation. **Sushmita Ghosh:** Writing – original draft, Methodology, Investigation. **Sutapa Mahata:** Writing – original draft, Methodology, Investigation, Formal analysis. **Vilas D. Nasare:** Supervision, Methodology, Investigation, Formal analysis, Data curation. **Ravikumar Kapavarapu:** Writing – original draft, Validation, Software. **Suresh Kumar:** Writing – review & editing, Supervision, Resources, Project administration, Conceptualization.

Declaration of competing interest

The authors declare that they have no known competing financial interests or personal relationships that could have appeared to influence the work reported in this paper.

Acknowledgement

The authors are thankful to Kurukshetra University Kurukshetra for providing lab facilities to carry out this work and the DST-FIST programme 2017 (SR/FST/CS-I/2017/12(C)) for providing NMR facility. This research did not receive any specific grants or financial support from public, commercial, or not-for-profit sectors.

Appendix A. Supplementary data

Supplementary data to this article can be found online at https://doi.org/10.1016/j.heliyon.2024.e26843.

References

[1] M.F. Khan, M.M. Alam, G. Verma, W. Akhtar, M. Akhter, M. Shaquiquzzaman, The therapeutic voyage of pyrazole and its analogs: a review, Eur. J. Med. Chem. 120 (2016) 170–201.
[2] G. Küçükgüzel Ş, S. Şenkardeş, Recent advances in bioactive pyrazoles, Eur. J. Med. Chem. 97 (2015) 786–815.
[3] J. García-Vanegas, A. Ramirez, A. Fuentes-Benítes, D. MartÍnez-Otero, N. González-Rivas, E. Cuevas-Yañez, Synthesis and in-vitro biological evaluation of 1,1-diaryl-2-(1,2,3)triazol-1-yl-ethanol derivatives as antifungal compounds flutriafol analogues, J. Chem. Sci. 131 (4) (2019) 1–10.
[4] N. Shah, N.M. Shah, M.P. Patel, R.G. Patel, Synthesis of 2-amino-4H-chromene derivatives under microwave irradiation and their antimicrobial activity, ChemInform 44 (2013).
[5] J.C. Jeyaveeran, C. Praveen, Y. Arun, A.A. M Prince, P.T. Perumal, Cycloisomerization of acetylenic oximes and hydrazones under gold catalysis: synthesis and cytotoxic evaluation of isoxazoles and pyrazoles, J. Chem. Sci. 128 (1) (2016) 73–83.
[6] P. Yadav, N.V. Purohit, Synthesis and evaluation of some bioactive compounds having oxygen and nitrogen heteroatom, J. Chem. Sci. 125 (1) (2013) 165–173.
[7] J. Burschka, A. Dualeh, F. Kessler, E. Baranoff, N.-L. Cevey-Ha, C. Yi, M.K. Nazeeruddin, M. Grätzel, Tris(2-(1H-pyrazol-1-yl)pyridine)cobalt(III) as p-type dopant for organic semiconductors and its application in highly efficient solid-state dye-sensitized solar cells, J. Am. Chem. Soc. 133 (45) (2011) 18042–18045.
[8] F. Giornal, S. Pazenok, L. Rodefeld, N. Lui, J.-P. Vors, F.R. Leroux, Synthesis of diversely fluorinated pyrazoles as novel active agrochemical ingredients, J. Fluor. Chem. 152 (2013) 2–11.
[9] A. Romero, E. Ramos, I. Ares, V. Castellano, M. Martínez, M.R. Martínez-Larrañaga, A. Anadón, M.A. Martínez, Fipronil sulfone induced higher cytotoxicity than fipronil in SH-SY5Y cells: protection by antioxidants, Toxicol. Lett. 252 (2016) 42–49.
[10] A.S. Hassan, G.O. Moustafa, A.A. Askar, A.M. Naglah, M.A. Al-Omar, Synthesis and antibacterial evaluation of fused pyrazoles and Schiff bases, Synth. Commun. 48 (21) (2018) 2761–2772.
[11] S. Chauhan, S. Paliwal, R. Chauhan, Anticancer activity of pyrazole via different biological mechanisms, Synth. Commun. 44 (10) (2014) 1333–1374.
[12] S. Deshmukh, K. Dingore, V. Gaikwad, M. Jachak, An efficient synthesis of pyrazolo[1,5-a]pyrimidines and evaluation of their antimicrobial activity, J. Chem. Sci. 128 (9) (2016) 1459–1468.
[13] M. Parshad, V. Verma, D. Kumar, B. Narasimhan, S. Kour, S. Singh, P.L. Sangwan, Iodobenzene diacetate-mediated isomerization of pyrazolyl chalcones and their cytotoxicity and anti-microbial activity, J. Chem. Sci. 127 (3) (2015) 413–423.
[14] M. Faisal, A. Saeed, S. Hussain, P. Dar, F.A. Larik, Recent developments in synthetic chemistry and biological activities of pyrazole derivatives, J. Chem. Sci. 131 (8) (2019) 1–30.
[15] S. Swami, A. Agarwala, B. Malik, R. Shrivastava, A new class of efficient 4-[(nitro substituted-phenyl)-hydrazonomethyl]-1-phenyl-1H-pyrazole-3-carboxylate derived colorimetric chemosensor for selective sensing of fluoride and other biologically important anions, J. Chem. Sci. 128 (9) (2016) 1451–1457.
[16] L.M. Blair, J. Sperry, Natural products containing a nitrogen–nitrogen bond, J. Nat. Prod. 76 (4) (2013) 794–812.
[17] V. Kumar, K. Kaur, G.K. Gupta, A.K. Sharma, Pyrazole containing natural products: synthetic preview and biological significance, Eur. J. Med. Chem. 69 (2013) 735–753.
[18] V.L.M. Silva, A.M.S. Silva, Recent advances in the synthesis, functionalization and applications of pyrazole-type compounds II&rdquo, Molecules 28 (15) (2023) 5873.
[19] M. Lusardi, A. Spallarossa, C. Brullo, Amino-Pyrazoles in medicinal chemistry: a review, Int. J. Mol. Sci. 24 (9) (2023) 7834.
[20] M. Mantzanidou, E. Pontiki, D. Hadjipavlou-Litina, Pyrazoles and pyrazolines as anti-inflammatory agents, Molecules 26 (11) (2021) 3439, 1-18.
[21] R.R. Ranatunge, R.A. Earl, D.S. Garvey, D.R. Janero, L.G. Letts, A.M. Martino, M.G. Murty, S.K. Richardson, D.J. Schwalb, D.V. Young, I.S. Zemtseva, 3-(2-Methoxytetrahydrofuran-2-yl)pyrazoles: a novel class of potent, selective cyclooxygenase-2 (COX-2) inhibitors, Bioorg, Med. Chem. Lett. 14 (24) (2004) 6049–6052.
[22] K. Ilango, P. Valentina, Textbook of Medicinal Chemistry, vol. 1, Keerthi Publishers, Chennai, 2007, pp. 336–352.
[23] A.A. Bekhit, H.M. Ashour, Y.S. Abdel Ghany, D. Bekhit Ael, A. Baraka, Synthesis and biological evaluation of some thiazolyl and thiadiazolyl derivatives of 1H-pyrazole as anti-inflammatory antimicrobial agents, Eur. J. Med. Chem. 43 (3) (2008) 456–463.
[24] E.K.A. Abdelall, G.M. Kamel, Synthesis of new thiazolo-celecoxib analogues as dual cyclooxygenase-2/15-lipoxygenase inhibitors: determination of regio-specific different pyrazole cyclization by 2D NMR, Eur. J. Med. Chem. 118 (2016) 250–258.
[25] S.D. Sawant, G. Lakshma Reddy, M.I. Dar, M. Srinivas, G. Gupta, P.K. Sahu, P. Mahajan, A. Nargotra, S. Singh, S.C. Sharma, M. Tikoo, G. Singh, R. A. Vishwakarma, S.H. Syed, Discovery of novel pyrazolopyrimidinone analogs as potent inhibitors of phosphodiesterase type-5, Bioorg, Med. Chem. 23 (9) (2015) 2121–2128.
[26] S. Rocha, M. Lucas, V.L. Silva, P.M. Gomes, A.M. Silva, A.N. Araújo, N. Aniceto, R.C. Guedes, M.L. Corvo, E. Fernandes, Pyrazoles as novel protein tyrosine phosphatase 1B (PTP1B) inhibitors: an in vitro and in silico study, Int. J. Biol. Macromol. 181 (2021) 1171–1182.
[27] Ş.G. Küçükgüzel, S. Şenkardeş, Recent advances in bioactive pyrazoles, Eur. J. Med. Chem. 97 (2015) 786–815.
[28] K. Karrouchi, S. Radi, Y. Ramli, J. Taoufik, Y.N. Mabkhot, F.A. Al-Aizari, M. Ansar, Synthesis and pharmacological activities of pyrazole derivatives: a review, Molecules 23 (1) (2018) 134.
[29] S.L. Tseng, M.S. Hung, C.P. Chang, J.S. Song, C.L. Tai, H.H. Chiu, W.P. Hsieh, Y. Lin, W.L. Chung, C.W. Kuo, C.H. Wu, C.M. Chu, Y.S. Tung, Y.S. Chao, K.S. Shia, Bioisosteric replacement of the pyrazole 5-aryl moiety of N-(piperidin-1-yl)-5-(4-chlorophenyl)-1-(2,4-dichlorophenyl)-4-methyl-1H-pyrazole-3-carboxamide (SR141716A). A novel series of alkynylthiophenes as potent and selective cannabinoid-1 receptor antagonists, J. Med. Chem. 51 (17) (2008) 5397–5412.
[30] F.K. Keter, J. Darkwa, Perspective: the potential of pyrazole-based compounds in medicine, Biometals : an international journal on the role of metal ions in biology, biochemistry, and medicine 25 (1) (2012) 9–21.
[31] F.E. Bennani, L. Doudach, Y. Cherrah, Y. Ramli, K. Karrouchi, M.E.A. Faouzi, Overview of recent developments of pyrazole derivatives as an anticancer agent in different cell line, Bioorg. Chem. 97 (2020) 103470.
[32] R. Verma, S.K. Verma, K.P. Rakesh, Y.R. Girish, M. Ashrafizadeh, K.S.S. Kumar, K.S. Rangappa, Pyrazole-based analogs as potential antibacterial agents against methicillin-resistance staphylococcus aureus (MRSA) and its SAR elucidation, Eur. J. Med. Chem. 212 (1–25) (2021) 113134.
[33] M. Ms Wassel, W.M. Gamal Eldin, A. Ragab, G. Am Elhag Ali, Y.A. Ammar, Antiviral activity of adamantane-pyrazole derivatives against foot and mouth disease virus infection in vivo and in vitro with molecular docking study, J. App. Vet. Sci. 5 (4) (2020) 37–46.

[34] L.R. Dias, M.B. Santos, S. de Albuquerque, H.C. Castro, A.M. de Souza, A.C. Freitas, M.A. DiVaio, L.M. Cabral, C.R. Rodrigues, Synthesis, in vitro evaluation, and SAR studies of a potential antichagasic 1H-pyrazolo [3, 4-b] pyridine series, Bioorg. Med. Chem. 15 (1) (2007) 211–219.

[35] M. Sánchez-Moreno, F. Gómez-Contreras, P. Navarro, C. Marín, I. Ramírez-Macías, F. Olmo, A.M. Sanz, L. Campayo, C. Cano, M.J. Yunta, In vitro leishmanicidal activity of imidazole- or pyrazole-based benzo[g]phthalazine derivatives against Leishmania infantum and Leishmania braziliensis species, J. Antimicrob. Chemother. 67 (2) (2012) 387–397.

[36] J. Wu, B.A. Song, D.Y. Hu, M. Yue, S. Yang, Design, synthesis and insecticidal activities of novel pyrazole amides containing hydrazone substructures, Pest Manag. Sci. 68 (5) (2012) 801–810.

[37] J.-J. Liu, M.-y. Zhao, X. Zhang, X. Zhao, H.-L. Zhu, Pyrazole derivatives as antitumor, anti-inflammatory and antibacterial agents, Mini-Rev. Med. Chem. 13 (13) (2013) 1957–1966.

[38] S. Mor, M. Khatri, R. Punia, S. Sindhu, Recent progress in anticancer agents incorporating pyrazole scaffold, Mini Rev. Med. Chem. 22 (1) (2022) 115–163.

[39] Y. Li, H. Zhao, C. Niu, H.A. Aisa, X. Hou, Synthesis and antimicrobial activity of aurone derivatives containing heterocyclic substituents, Russ. J. Gen. Chem. 92 (8) (2022) 1562–1573.

[40] R. Fioravanti, A. Bolasco, F. Manna, F. Rossi, F. Orallo, F. Ortuso, S. Alcaro, R. Cirilli, Synthesis and biological evaluation of N-substituted-3,5-diphenyl-2-pyrazoline derivatives as cyclooxygenase (COX-2) inhibitors, Eur. J. Med. Chem. 45 (12) (2010) 6135–6138.

[41] S.K. Cox, J. Roark, A. Gassel, K. Tobias, Determination of deracoxib in feline plasma samples using high performance liquid chromatography, J. Chromatogr. B 819 (1) (2005) 181–184.

[42] G.S. Hassan, S.M. Abou-Seri, G. Kamel, M.M. Ali, Celecoxib analogs bearing benzofuran moiety as cyclooxygenase-2 inhibitors: design, synthesis and evaluation as potential anti-inflammatory agents, Eur. J. Med. Chem. 76 (2014) 482–493.

[43] C.M. Boustany-Kari, V.M. Jackson, C.P. Gibbons, A.G. Swick, Leptin potentiates the anti-obesity effects of rimonabant, Eur. J. Pharmacol. 658 (2) (2011) 270–276.

[44] P.R. Wyde, B.E. Gilbert, M.W. Ambrose, Comparison of the anti-respiratory syncytial virus activity and toxicity of papaverine hydrochloride and pyrazofurin in vitro and in vivo, Antivir. Res. 11 (1) (1989) 15–26.

[45] T. Kameyama, T. Nabeshima, Effects of 1,3-diphenyl-5-(2-dimethylaminopropionamide)-pyrazole[difenamizole] on a conditioned avoidance response, Neuropharmacology 17 (4–5) (1978) 249–256.

[46] K.D. Ardern, F.S. Ram, Tartrazine exclusion for allergic asthma, Cochrane Database Syst. Rev. 4 (2001) (2001) Cd000460.

[47] G.M. Giancarlo, K. Venkatakrishnan, B.W. Granda, L.L. von Moltke, D.J. Greenblatt, Relative contributions of CYP2C9 and 2C19 to phenytoin 4-hydroxylation in vitro: inhibition by sulfaphenazole, omeprazole, and ticlopidine, Eur. J. Clin. Pharmacol. 57 (1) (2001) 31–36.

[48] K.S. Gould, C. Lister, Flavonoid functions in plants, in: BOOK: Flavonoids: Chemistry, Biochemistry and Applications, 2006, pp. 397–441.

[49] E. Lathwal, S. Kumar, A review of the various synthetic approaches to access aurone derivatives and their biological activities, Curr. Org. Chem. 27 (4) (2023) 308–351.

[50] A.N. Panche, A.D. Diwan, S.R. Chandra, Flavonoids: an overview, J. Nutr. Sci. 5 (e47) (2016) 1–15.

[51] T.A. Geissman, J.B. Harborne, Anthochlor pigments. XIII. The ultraviolet absorption spectra of phenolic plant pigments. Polyhydroxyaurones, J. Am. Chem. Soc. 78 (4) (1956) 832–837.

[52] J.B. Harborne, BOOK the Flavonoids: Advances in Research since 1980, 2013.

[53] G. Kumar, E. Lathwal, B. Saroha, S. Kumar, S. Kumar, N.S. Chauhan, T. Kumar, Synthesis and Biological Evaluation of Quinoline-Based Novel Aurones, ChemistrySelect 5 (12) (2020) 3539–3543.

[54] R. Alghazeer, F. Whida, E. Abduelrhman, F. Gammoudi, S. Azwai, Screening of antibacterial activity in marine green, red and brown macroalgae from the western coast of Libya, Nat. Sci. 5 (1) (2013) 7–14.

[55] C.-Y. Lee, E.-H. Chew, M.-L. Go, Functionalized aurones as inducers of NAD(P)H:quinone oxidoreductase 1 that activate AhR/XRE and Nrf2/ARE signaling pathways: synthesis, evaluation and SAR, Eur. J. Med. Chem. 45 (7) (2010) 2957–2971.

[56] C.Y. Lee, E.H. Chew, M.L. Go, Functionalized aurones as inducers of NAD(P)H:quinone oxidoreductase 1 that activate AhR/XRE and Nrf2/ARE signaling pathways: synthesis, evaluation and SAR, Eur. J. Med. Chem. 45 (7) (2010), 2957-2571.

[57] E.H. Lee, D.G. Song, J.Y. Lee, C.H. Pan, B.H. Um, S.H. Jung, Inhibitory effect of the compounds isolated from Rhus verniciflua on aldose reductase and advanced glycation endproducts, Biol. Pharm. Bull. 31 (8) (2008) 1626–1630.

[58] A. Detsi, M. Majdalani, C.A. Kontogiorgis, D. Hadjipavlou-Litina, P. Kefalas, Natural and synthetic 2′-hydroxy-chalcones and aurones: synthesis, characterization and evaluation of the antioxidant and soybean lipoxygenase inhibitory activity, Bioorg. Med. Chem. 17 (23) (2009) 8073–8085.

[59] M.P. Carrasco, A.S. Newton, L. Gonçalves, A. Góis, M. Machado, J. Gut, F. Nogueira, T. Hänscheid, R.C. Guedes, D.J.V.A. dos Santos, P.J. Rosenthal, R. Moreira, Probing the aurone scaffold against Plasmodium falciparum: design, synthesis and antimalarial activity, Eur. J. Med. Chem. 80 (2014) 523–534.

[60] B.P. Bandgar, S.A. Patil, B.L. Korbad, S.C. Biradar, S.N. Nile, C.N. Khobragade, Synthesis and biological evaluation of a novel series of 2,2-bisaminomethylated aurone analogues as anti-inflammatory and antimicrobial agents, Eur. J. Med. Chem. 45 (7) (2010) 3223–3227.

[61] M. Morimoto, H. Fukumoto, T. Nozoe, A. Hagiwara, K. Komai, Synthesis and insect antifeedant activity of aurones against spodoptera litura larvae, J. Agric. Food Chem. 55 (3) (2007) 700–705.

[62] S. Nigam, B.S. Jayashree, Limitation of Algar–Flynn–Oyamada reaction using methoxy substituted chalcones as reactants and evaluation of the newly transformed aurones for their biological activities, Res. Chem. Intermed. 43 (5) (2017) 2839–2864.

[63] D. Ashok, K. Rangu, S. Gundu, A. Lakkadi, P. Tigulla, Microwave-assisted synthesis, molecular docking, and biological evaluation of 2-arylidene-2H-furo[2,3-f] chromen-3(7H)-ones as antioxidant and antimicrobial agents, Med. Chem. Res. 26 (8) (2017) 1735–1746.

[64] M. Ono, R. Ikeoka, H. Watanabe, H. Kimura, T. Fuchigami, M. Haratake, H. Saji, M. Nakayama, 99mTc/Re complexes based on flavone and aurone as SPECT probes for imaging cerebral β-amyloid plaques, Bioorg. Med. Chem. Lett 20 (19) (2010) 5743–5748.

[65] N.N. Agrawal, P.A. Soni, A new process for the synthesis of aurones by using mercury (II) acetate in pyridine and cupric bromide in dimethyl sulfoxide, ChemInform 37 (39) (2006) no-no.

[66] T. Narsinghani, M.C. Sharma, S. Bhargav, Synthesis, docking studies and antioxidant activity of some chalcone and aurone derivatives, Med. Chem. Res. 22 (9) (2013) 4059–4068.

[67] G. Kumar, B. Saroha, R. Kumar, M. Kumari, S. Kumar, Recent advances in synthesis and biological assessment of quinoline-oxygen heterocycle hybrids, ChemistrySelect 6 (20) (2021) 5148–5165.

[68] N.N. Agrawal, P.A. Soni, A new process for the synthesis of aurones by using mercury (II) acetate in pyridine and cupric bromide in dimethyl sulfoxide, ChemInform 37 (39) (2006).

[69] Y. Li, X. Qiang, L. Luo, Y. Li, G. Xiao, Z. Tan, Y. Deng, Synthesis and evaluation of 4-hydroxyl aurone derivatives as multifunctional agents for the treatment of Alzheimer's disease, Bioorg. Med. Chem. 24 (10) (2016) 2342–2351.

[70] Y. Lv, Z. Zheng, R. Liu, J. Guo, C. Zhang, Y. Xie, Monoamine oxidase B inhibitors based on natural privileged scaffolds: a review of systematically structural modification, Int. J. Biol. Macromol. 251 (2023) 126158.

[71] S. Shrestha, S. Natarajan, J.H. Park, D.Y. Lee, J.G. Cho, G.S. Kim, Y.J. Jeon, S.W. Yeon, D.C. Yang, N.I. Baek, Potential neuroprotective flavonoid-based inhibitors of CDK5/p25 from Rhus parviflora, Bioorg. Med. Chem. Lett 23 (18) (2013) 5150–5154.

[72] Y.H. Lee, M.C. Shin, Y.D. Yun, S.Y. Shin, J.M. Kim, J.M. Seo, N.J. Kim, J.H. Ryu, Y.S. Lee, Synthesis of aminoalkyl-substituted aurone derivatives as acetylcholinesterase inhibitors, Bioorg. Med. Chem. 23 (1) (2015) 231–240.

[73] S. Okombi, D. Rival, S. Bonnet, A.M. Mariotte, E. Perrier, A. Boumendjel, Discovery of benzylidenebenzofuran-3(2H)-one (aurones) as inhibitors of tyrosinase derived from human melanocytes, J. Med. Chem. 49 (1) (2006) 329–333.

[74] W. Zhao, J. Sun, H. Xiang, Y.Y. Zeng, X.B. Li, H. Xiao, D.Y. Chen, R.L. Ma, Synthesis and biological evaluation of new flavonoid fatty acid esters with anti-adipogenic and enhancing glucose consumption activities, Bioorg. Med. Chem. 19 (10) (2011) 3192–3203.

[75] J. Ma, S.H. Jones, S.M. Hecht, A coumarin from Mallotus resinosus that mediates DNA cleavage, J. Nat. Prod. 67 (9) (2004) 1614–1616.

[76] Y. Xie, L.M. Kril, T. Yu, W. Zhang, M.S. Frasinyuk, S.P. Bondarenko, K.M. Kondratyuk, E. Hausman, Z.M. Martin, P.P. Wyrebek, X. Liu, A. Deaciuc, L.P. Dwoskin, J. Chen, H. Zhu, C.-G. Zhan, V.M. Sviripa, J. Blackburn, D.S. Watt, C. Liu, Semisynthetic aurones inhibit tubulin polymerization at the colchicine-binding site and repress PC-3 tumor xenografts in nude mice and myc-induced T-ALL in zebrafish, Sci. Rep. 9 (1) (2019) 6439–6453.
[77] A. Boumendjel, C. Beney, N. Deka, A.M. Mariotte, M.A. Lawson, D. Trompier, H. Baubichon-Cortay, A. Di Pietro, 4-Hydroxy-6-methoxyaurones with high-affinity binding to cytosolic domain of P-glycoprotein, Chem. Pharm. Bull. (Tokyo) 50 (6) (2002) 854–856.
[78] A.A.M. Alkhaldi, M.M. Al-Sanea, A. Nocentini, W.M. Eldehna, Z.M. Elsayed, A. Bonardi, M.F. Abo-Ashour, A.K. El-Damasy, M.S. Abdel-Maksoud, T. Al-Warhi, P. Gratteri, H.A. Abdel-Aziz, C.T. Supuran, R. El-Haggar, 3-Methylthiazolo[3,2-a]benzimidazole-benzenesulfonamide conjugates as novel carbonic anhydrase inhibitors endowed with anticancer activity: design, synthesis, biological and molecular modeling studies, Eur. J. Med. Chem. 207 (2020) 112745.
[79] H.M. Sim, C.P. Wu, S.V. Ambudkar, M.L. Go, In vitro and in vivo modulation of ABCG2 by functionalized aurones and structurally related analogs, Biochem. Pharmacol. 82 (11) (2011) 1562–1571.
[80] B. Saroha, G. Kumar, P. Arya, N. Raghav, S. Kumar, Some morpholine tethered novel aurones: design, synthesis, biological, kinetic and molecular docking studies, Bioorg. Chem. 140 (2023) 106805.
[81] M. Roussaki, S. Costa Lima, A.M. Kypreou, P. Kefalas, A. Cordeiro da Silva, A. Detsi, Aurones: a promising heterocyclic scaffold for the development of potent antileishmanial agents, International journal of medicinal chemistry 2012 (2012) 196921.
[82] O.V. Muzychka, O.L. Kobzar, A.V. Popova, M.S. Frasinyuk, A.I. Vovk, Carboxylated aurone derivatives as potent inhibitors of xanthine oxidase, Bioorg. Med. Chem. 25 (14) (2017) 3606–3613.
[83] K.F. Liew, K.L. Chan, C.Y. Lee, Blood-brain barrier permeable anticholinesterase aurones: synthesis, structure-activity relationship, and drug-like properties, Eur. J. Med. Chem. 94 (2015) 195–210.
[84] Y.-T. Bao, M. Zhang, T. Li, H.-F. Xiao, T. Zhao, X.-H. Xu, L.-Q. Yang, Synthesis and biological activities of 6-hydroxyaurone derivatives, J. Heterocycl. Chem. 53 (2) (2016) 637–642.
[85] X. Zheng, J.-G. Cao, W.-D. Meng, F.-L. Qing, Synthesis and anticancer effect of B-Ring trifluoromethylated flavonoids, Bioorg. Med. Chem. Lett. 13 (20) (2003) 3423–3427.
[86] E. Lathwal, S. Kumar, P. Kumar Sahoo, S. Ghosh, S. Mahata, V.D. Nasare, S. Kumar, Synthesis, cytotoxic evaluation and structure activity relationship of pyrazole hybrid aurones on gastric cancer (AGS) cell lines, Results Chem 4 (1–11) (2022) 100590.
[87] C.F. Silva, D.C. Pinto, A.M. Silva, Chromones: privileged scaffolds for the production of multi-target-directed-ligand agents for the treatment of Alzheimer's disease, Expet Opin. Drug Discov. 13 (12) (2018) 1141–1151.
[88] L. Jalili-Baleh, E. Babaei, S. Abdpour, S.N.A. Bukhari, A. Foroumadi, A. Ramazani, M. Sharifzadeh, M. Abdollahi, M. Khoobi, A review on flavonoid-based scaffolds as multi-target-directed ligands (MTDLs) for Alzheimer's disease, Eur. J. Med. Chem. 152 (2018) 570–589.
[89] L. Pinzi, G. Rastelli, Molecular docking: shifting paradigms in drug discovery, Int. J. Mol. Sci. 20 (18) (2019) 4331.
[90] C. Gravalos, A. Jimeno, HER2 in gastric cancer: a new prognostic factor and a novel therapeutic target, Ann. Oncol. 19 (9) (2008) 1523–1529.
[91] H. Lote, I. Chau, Emerging HER2-directed therapeutic agents for gastric cancer in early phase clinical trials, Expet Opin. Invest. Drugs 31 (1) (2022) 59–78.
[92] S. Kumar, An improved one-pot and eco-friendly synthesis of aurones under solvent-free conditions, Green Chem. Lett. Rev. 7 (1) (2014) 95–99.
[93] S. Kumar, E. Lathwal, G. Kumar, B. Saroha, S. Kumar, S. Mahata, P.K. Sahoo, V.D. Nasare, Synthesis of pyrazole based novel aurone analogs and their cytotoxic activity against MCF-7 cell line, Chem. Data Collect. 30 (2020) 100559.
[94] A.A. Elhadi, H. Osman, M.A. Iqbal, S.K. Rajeswari, M.B.K. Ahamed, A.M.S. Abdul Majid, M.M. Rosli, I.A. Razak, A.S.A. Majid, Synthesis and structural elucidation of two new series of aurone derivatives as potent inhibitors against the proliferation of human cancer cells, Med. Chem. Res. 24 (9) (2015) 3504–3515.
[95] J.M. Yang, C.C. Chen, GEMDOCK: a generic evolutionary method for molecular docking, Proteins 55 (2) (2004) 288–304.
[96] K. Aertgeerts, R. Skene, J. Yano, B.C. Sang, H. Zou, G. Snell, A. Jennings, K. Iwamoto, N. Habuka, A. Hirokawa, T. Ishikawa, T. Tanaka, H. Miki, Y. Ohta, S. Sogabe, Structural analysis of the mechanism of inhibition and allosteric activation of the kinase domain of HER2 protein, J. Biol. Chem. 286 (21) (2011) 18756–18765.
[97] J.-M. Yang, Development and evaluation of a generic evolutionary method for protein–ligand docking, J. Comput. Chem. 25 (6) (2004) 843–857.
[98] C. Fong, I. Chau, HER2 inhibition in gastric cancer-novel therapeutic approaches for an established target, Cancers 14 (15) (2022) 3824, 1-20.
[99] A. Daina, O. Michielin, V. Zoete, SwissADME: a free web tool to evaluate pharmacokinetics, drug-likeness and medicinal chemistry friendliness of small molecules, Sci. Rep. 7 (1) (2017) 42717.